

Thermal conductivity
at very low temperatures

J. N. Haasbroek

Universiteit Leiden



1 400 169 2

BIBLIOSERIE

PHYSIQUES LABORATORIA

NUMM. 3592

2300 BA, LEIDEN

TELEFON: 547 4066/67

Thermal conductivity at very low temperatures

STELLINGEN

Stellingen van het proefschrift van

J. N. H. H. H. H.

STELLINGEN

behorende bij het proefschrift van

J.N. Haasbroek

1. De Debye temperatuur θ_D wordt vaak afgeleid uit soortelijke warmte metingen bij lage temperatuur; voor dat geval zijn twee definities van θ_D in gebruik. Die definitie waarbij het aantal atomen c.q. atoomgroepen in de eenheidscel in rekening wordt gebracht, verdient de voorkeur.
2. Voor de ijking van meetmethoden van de warmtegeleiding bij zeer lage temperatuur zijn LiF kristallen aan te bevelen als standaardmateriaal.
3. De door Wolfmeier en Dillinger gesignaleerde overeenkomst tussen de gemeten warmtegeleiding in Al_2O_3 en de door hen berekende waarde berust slechts op een samenloop van omstandigheden.
M.W. Wolfmeier and J.R. Dillinger, Phys. Letters 34A (1971) 247.
4. Er zijn aanwijzingen dat in een driedimensionale Heisenberg ferromagneet de warmtegeleiding door magnetische excitaties, dan wel de afgeleide naar de temperatuur daarvan, discontinu is bij de faseovergang.
5. Het gedrag van de warmtegeleiding nabij een magnetische faseovergang kan als functie van de temperatuur en tevens als functie van het magneetveld worden bestudeerd; het laatste verdient veelal de voorkeur.
6. De temperatuurafhankelijkheid van de warmtegeleiding van FeCl_2 nabij T_N wordt veeleer bepaald door het transport van magnetische excitaties, dan door kritische fluctuaties in het spinsysteem.
G. Laurence, Phys. Letters 34A (1971) 308.
7. Het is mogelijk dat de warmteweerstand van het grensvlak tussen twee (bijvoorbeeld para-) magnetische zouten een ander karakter heeft dan die tussen diamagnetische zouten.
8. Het is te verwachten dat de absorptiecoëfficiënt voor ultrageluid in $\text{Cu}(\text{NH}_4)_2\text{Br}_4 \cdot 2\text{H}_2\text{O}$ bij de ferromagnetische faseovergang niet divergeert, doch eindig blijft en sterk toeneemt beneden T_C .

9. In een geschikt gekozen combinatie van halfgeleiders zou, bij het grensvlak, een monochromatische fononenbundel kunnen worden opgewekt.
10. Met een experiment analoog aan de proef van Young zou interferentie van warmtegolven in een kristal kunnen worden aangetoond.
11. Het is wenselijk een permanente, van inhoud variërende, tentoonstelling over het wetenschappelijk onderzoek aan de universiteiten in te richten.
12. Het is wenselijk werkbezoeken aan een universiteit op te nemen in het programma van de hogere klassen van de middelbare scholen. De universiteit zou hiertoe faciliteiten ter beschikking moeten stellen.
13. Een visie op het geheel is nodig wanneer men details wil interpreteren; dit leidt bij wetenschappelijk onderzoek tot het werken met modellen, en bij nieuwsmedia tot (dus niet laakbare) tendentieuze voorlichting.
14. De vrijheid tot meningsuiting en meningsvorming wordt verwezenlijkt door middel van onderwijs, gesprekken, pers, radio en televisie. Van deze komt alleen de pers tot stand binnen een commerciële organisatie. Gezien de huidige ontwikkeling bij de dagbladpers is het de hoogste tijd dat deze uitzonderingspositie wordt opgeheven.
15. Bij de huidige opzet van de kindbescherming schuilt in de 'uithuisplaatsing' een risico van het buiten de maatschappij plaatsen. De aanpak waarbij de kinderen met hun groepsleiders een gezin vormen in een gewoon huis in een gewone straat zou hiervoor een oplossing kunnen brengen.

'Browndale' de Groene 13-3-1971.

1. The first step in the process of the...
2. The second step is to identify the...
3. The third step is to analyze the...
4. The fourth step is to evaluate the...
5. The fifth step is to implement the...
6. The sixth step is to monitor the...
7. The seventh step is to report the...
8. The eighth step is to review the...
9. The ninth step is to improve the...
10. The tenth step is to conclude the...

Thermal conductivity at very low temperatures

PROEFSCHRIFT

TER VERKRIJGING VAN DE GRAAD VAN DOCTOR
IN DE WISKUNDE EN NATUURWETENSCHAPPEN AAN
DE RIJKSUNIVERSITEIT TE LEIDEN, OP GEZAG VAN
DE RECTOR MAGNIFICUS DR. C. SOETEMAN, HOOG-
LERAAR IN DE FACULTEIT DER LETTEREN, TEN
OVERSTAAN VAN EEN COMMISSIE UIT DE SENAAT
TE VERDEDIGEN OP WOENSDAG 30 JUNI 1971
TE KLOKKE 14.15 UUR

DOOR

JACOB NICOLAAS HAASBROEK

GEBOREN TE 's-GRAVENHAGE IN 1941

DRUK: elve/labor vincit

PROMOTOR: DR. C.J. GORTER

Werkgroepleider: dr. W.J. Huiskamp

Op verzoek van de Faculteit der Wiskunde en Natuurwetenschappen volgt hier een kort overzicht van mijn studie.

Na de HBS-B opleiding aan het Christelijk Lyceum 'Zandvliet' te 's-Gravenhage begon ik in 1958 mijn studie aan de Rijksuniversiteit te Leiden. Het kandidaatsexamen met de hoofdvakken natuurkunde en wiskunde en bijvak scheikunde is in 1962 afgelegd. Hierop volgde in 1965 het doctoraal examen experimentele natuurkunde met bijvak mechanica. Sinds november 1962 ben ik werkzaam op het Kamerlingh Onnes laboratorium in de werkgroep adiabatische demagnetisatie en kernfysica, waarvan dr. W.J. Huiskamp de leiding heeft. Prof. dr. A.R. Miedema en dr. H. van Kempen hebben mij ingewijd in de geheimen van de experimentele natuurkunde bij zeer lage temperaturen.

De Stichting voor Fundamenteel Onderzoek der Materie heeft mij een kandidaatsassistent-schap in de werkgroep K IV verleend vanaf juli 1963. Sinds december 1965 ben ik, als wetenschappelijk medewerker, in dienst van de Rijksuniversiteit Leiden.

Vanaf 1963 heb ik, in verschillende functies, medewerking verleend aan het natuurkunde-praktikum. De bestuurlijke kant van de universiteit heb ik leren kennen als vertegenwoordiger van de wetenschappelijke staf.

Velen hebben bijgedragen tot het welslagen van het onderzoek vermeld in dit proefschrift, ik wil hen hartelijk danken voor hun medewerking. In het bijzonder een woord van dank aan de heren J. van Weesel, J. van der Waals en R. Hulstman, die door raad en daad veel technische problemen uit de weg hebben geruimd. In de loop der jaren heb ik de hulp gehad van vele medewerkers. De enthousiaste inzet van de heren J.A. Konter, drs. N. de Boo en A.S.M. Gieske zij hier met eer vermeld.

Veel profijt heb ik gehad van de discussies met dr. W.J. Huiskamp, die het manuscript van kritische opmerkingen voorzag. Erkentelijk ben ik dr. R.C. Tiel voor correcties op mijn Engels taalgebruik, mejuffrouw M.H. van Kerkhoven voor het typen van het manuscript en de heren H.J. Rijskamp en W.F. Tegelaar voor het verzorgen van de figuren.

CONTENTS

INTRODUCTION AND SURVEY	11
CHAPTER I Introduction to low temperature thermal conductivity	
I.1 Lattice conductivity	15
I.2 A simple model for phonon scattering in a magnetic crystal	19
I.3 Experimental requirements	22
I.4 Method for measuring thermal conductivity below 1 Kelvin	22
I.5 Equilibrium time of the process	25
I.6 Some experimental results	26
I.7 Discussion of the method	34
CHAPTER II Cryostat covering the temperature range $0.05 < T < 5$ K	
II.1 The cryostat and ^3He system	37
II.2 The superconducting magnet	38
II.3 The cooling salt	41
II.4 The thermal contact between ^3He and cooling salt	41
II.5 Apparatus mounting and sample holder	45
CHAPTER III Temperature measurement and controle	
III.1 Carbon resistance thermometry	47
III.2 Procedure of the measurement	49
III.3 R - T calibration and magnetic thermometry	51
III.4 Magnetic field dependence of Speer resistors	53
CHAPTER IV Some considerations concerning the experimental results	
IV.1 Calibration and test of the procedure	55
IV.2 Thermal conductivity of He gas and its use as thermal switch	62
IV.3 Thermal conductivity in magnetic crystals	64
CHAPTER V Thermal conductivity of a 3D Heisenberg ferromagnet	
V.1 Scaling of the thermal conductivity near a magnetic phase transition	75
V.2 Thermal conductivity near a magnetic phase transition, comparison with a microscopic model	79
CONCLUDING REMARKS	85

SAMENVATTING

Warmtegeleiding bij zeer lage temperatuur is een tot nu toe weinig onderzocht gebied van de natuurkunde der vaste stof. Dit is waarschijnlijk een gevolg van het feit dat de warmtegeleiding bij lage temperatuur in het algemeen op eenvoudige wijze wordt beschreven. Deze eenvoudige beschrijving betreft dan kristaltrillingen (fononen) en, in een metaal, vrije electronen. Maar naast deze gebruikelijke transportmechanismen kunnen ook andere thermische excitaties een rol spelen. Dit komt in de warmtegeleiding tot uiting hetzij als een verlaging door extra fonon-verstrooiing, dan wel als een verhoging door transport ten gevolge van deze excitaties. In principe kunnen deze effecten zowel in dielectrische kristallen als in metalen bij willekeurige temperatuur worden bestudeerd. In dit proefschrift hebben we ons beperkt tot het onderzoek van de warmtegeleiding bij lage temperatuur in magnetische dielectrische kristallen, om op deze wijze te trachten thermische excitaties in een magnetisch spin systeem te onderzoeken.

Warmte-transport door thermische excitaties in een magnetisch systeem werd respectievelijk voor een paramagneet door Fröhlich en Heitler¹, en voor een ferromagneet door Sato² voorspeld. Van Kempen³ vermeldt een aantal warmtegeleidingsmetingen bij zeer lage temperatuur, met als belangrijkste resultaten dat de metingen aan waterhoudende kristallen reproduceren, en dat in een aantal gevallen de warmtegeleiding inderdaad wordt beïnvloed door de aanwezigheid van een magnetisch spin systeem. Het voorgaande was de aanzet voor het onderzoek dat in dit proefschrift is vermeld. Het hoofdonderwerp kon echter pas worden aangevat nadat een geschikte methode voor warmtegeleidingsmetingen bij zeer lage temperatuur was ontworpen.

In I.4 is de 'switchmethode' beschreven, welke geschikt is voor metingen bij temperaturen lager dan 1 K; de resultaten (I.6) bevestigen de conclusies van Van Kempen. Uit een nadere bespreking van de switchmethode (zie I.7) blijkt dat deze methode een aantal ongewenste beperkingen aan de meetmogelijkheden oplegt. Deze overwegingen leidden tot een nieuwe opzet voor de warmtegeleidingsmetingen, waarbij een groter temperatuurgebied wordt bestreken, en tevens magneetveldafhankelijkheid kan worden gemeten. Vooral de laatstgenoemde uitbreiding van de mogelijkheden bleek van groot belang voor de interpretatie van de metingen aan magnetische kristallen.

Hoofdstuk II beschrijft de opstelling voor het temperatuurgebied $0.05 < T < 5$ K. Dit temperatuurgebied wordt bestreken door koeling met zowel vloeibaar ³He als adiabatische

demagnetisatie. Voor de, in een dergelijke opzet noodzakelijke, warmte-schakelaar tussen de twee koelmethode is ^4He gas toegepast. Deze zogenoemde gas-switch is beschreven in II.4; metingen van de warmtegeleiding in een dergelijke constructie worden besproken in IV.2. De, in het temperatuurgebied beneden 1 K gebruikelijke, magnetische thermometrie is onhandelbaar als er in magneetveld wordt gemeten. Een alternatief is thermometrie op basis van de temperatuurafhankelijke elektrische weerstand van met name koolweerstand. De bij koolweerstandsthermometrie optredende problemen, de ijking als functie van magneetveld en temperatuur, en de gebruikte procedure voor warmtegeleidingsmetingen worden besproken in hoofdstuk III.

Een aantal experimentele resultaten worden besproken in hoofdstuk IV. In IV.1 zijn de testmetingen vermeld, waarbij zowel de absolute waarde, als de resulterende temperatuur- en magneetveldafhankelijkheid van de warmtegeleidingsmeting is gecontroleerd. De experimentele resultaten met LiF, verkregen in temperatuurgebied van 0.08 - 1.4 K, stemmen overeen met de theoretisch voorspelde temperatuurafhankelijkheid⁴. De theoretische absolute waarde blijkt echter een factor 2 groter te zijn dan de experimentele waarde. Dit leidde tot het uitgangspunt, verwerkt in dit proefschrift, dat de theoretische warmtegeleiding in het ' T^3 gebied' moet worden gereduceerd met een factor $\frac{1}{s}$, waarbij s wordt bepaald door het aantal atomen, c.q. atoomgroepen (NH_4 , H_2O e.d.) in het molecuul van de beschouwde stof. Dit uitgangspunt is, als voorbeeld, toegepast op de warmtegeleiding van $\text{ZnSiF}_6 \cdot 6\text{H}_2\text{O}$. De experimenteel gevonden waarde voor s (16 ± 3) stemt goed overeen met de gegeven definitie van s ($= 14$ voor $\text{ZnSiF}_6 \cdot 6\text{H}_2\text{O}$).

Het hoofdonderwerp van dit proefschrift betreft de warmtegeleiding van een aantal magnetische zouten, die zowel als functie van het magneetveld als van de temperatuur is bestudeerd (IV.3). De meeste resultaten hebben betrekking op kristallen met een magnetische fase-overgang in het beschouwde temperatuurgebied. De warmtegeleiding van CoCs_3Cl_5 (representant voor het 3D Ising-model) blijkt onafhankelijk van de fase-overgang. De warmtegeleiding van $\text{Cu}(\text{NH}_4)_2\text{Cl}_4 \cdot 2\text{H}_2\text{O}$ en $\text{Cu}(\text{NH}_4)_2\text{Br}_4 \cdot 2\text{H}_2\text{O}$ (representanten voor het 3D Heisenberg-model) wordt daarentegen sterk beïnvloed door de fase-overgang, resulterend in een minimum in de geleiding nabij T_c . Ook in de warmtegeleiding van $\text{Ni}_3\text{La}_2(\text{NO}_3)_{12} \cdot 24\text{H}_2\text{O}$ komt de fase-overgang duidelijk tot uiting, in dit geval echter als een toename van de fononverstrooiing beneden T_c . De magneetveldafhankelijkheid van de warmtegeleiding bleek een belangrijk gegeven te verschaffen voor de interpretatie van de resultaten. In de koperzouten kon, dank zij de metingen in magneetveld, warmte-transport in het magnetische spin systeem worden aangetoond.

Hoewel de literatuur over het gedrag van transportgrootheden bij een (magnetische) fase-overgang snel uitbreidt, zijn er tot nu toe slechts zeer weinig voorspellingen aangaande het gedrag van de warmtegeleiding bij een fase-overgang. Gezien de significante resultaten met de koperzouten leek het gewenst speciale aandacht te besteden aan de temperatuurafhankelijkheid van de warmtegeleiding in de nabijheid van de fase-overgang. Dit is beschreven in hoofdstuk V. De behandeling in V.1 is vooral fenomenologisch (dynamic scaling); in V.2

zijn de resultaten van $\text{Cu}(\text{NH}_4)_2\text{Cl}_4 \cdot 2\text{H}_2\text{O}$ vergeleken met een theoretisch model⁵. Voor $T > T_c$ wordt de fononvrije weglengte in eerste instantie bepaald door een proces dat omgekeerd evenredig is met de warmtegeleiding van het magnetische spin systeem. Als dit proces ook in de geordende toestand domineert, dient de warmtegeleiding van $\text{Cu}(\text{NH}_4)_2\text{Cl}_4 \cdot 2\text{H}_2\text{O}$ voor $T < T_c$ te worden toegeschreven aan warmte-transport door spin-golven. De resultaten (IV.2) en de nadere analyse (V) tonen aan dat warmtegeleidingsmetingen bruikbaar zijn voor het onderzoek van excitaties in een magnetisch spin systeem; mogen zij een uitnodiging zijn tot verder onderzoek van de warmtegeleiding bij zeer lage temperatuur.

Referenties

1. H. Fröhlich and W. Héitler, Proc. Roy. Soc. A 135 (1966) 640.
2. H. Sato, Progr. Theor. Phys. Kyoto 13 (1955) 119.
3. H. van Kempen, Thesis Leiden (1965).
4. H.B.G. Casimir, Physica 5 (1938) 495.
5. K. Kawasaki, Progr. Theor. Phys. 29 (1963) 801.

INTRODUCTION AND SURVEY

Thermal conductivity at very low temperatures, as treated in most textbooks on solid state physics, is expected to show a quite simple behaviour. The question, as to why there is a need for a thesis pertaining to the measurement of thermal conductivity at very low temperatures, may therefore be posed quite legitimately. However, an examination of the literature shows that very little experimental evidence exists for this postulated simple behaviour. Moreover, the above mentioned behaviour is to be expected only for thermal transport due to either electrons or vibrations of the atoms constituting the solid; and, as shown in this thesis, thermal energy carriers different from these may be effective as well. Actually, instead of being simple, a wide variety in temperature dependence and /or absolute values of the thermal conductivity may occur, even at very low temperature.

Experimentally, the thermal conductivity λ is, apart from a geometry factor L/S , defined as the proportionality constant between the heat flow \dot{Q} and the corresponding temperature difference ΔT along the sample, hence $\lambda = \frac{L}{S} \frac{\dot{Q}}{\Delta T}$.

Theoretically, thermal conductivity in a solid can be understood in the following way.

A solid may be regarded as an ideal crystal at rest with certain thermal excitations. If these excitations are free to move through the crystal, they give rise to thermal transport. The dispersion relation of these excitations leads to the thermodynamic quantities.

The easiest way to arrive at an expression for λ is to treat the excitations as the particles of an ideal gas. In that case, thermal transport is described by the well-known formula of the kinetic gas theory

$$\lambda = \frac{1}{3} c v l,$$

where c is the specific heat per unit volume, v the mean velocity and l the mean free path of the particles.

Similarly, for a solid with various excitations i one can write

$$\lambda = \frac{1}{3} \sum_i c_i v_i l_i.$$

In an actual solid, both c_i and l_i may be strongly temperature dependent. Furthermore, the mean free path will be determined by lattice defects, impurities, crystal size, and last but not least, by interactions between excitations of the same and/or different kind. Hence λ depends on both the substance and the particular sample chosen for the λ measurements.

The purpose of the experiments described in this thesis is an investigation of thermal excitations in a magnetic system and their interactions in a solid. In principle, one can measure these effects both in dielectric crystals and in metals and at arbitrary temperatures. Dielectric crystals were chosen since in that case the dominant excitations are usually lattice vibrations only, while in metals both lattice vibrations and electrons have always to be taken into account. Low temperatures are preferred since, as will be shown, the heat transport by lattice vibrations is quite simple to describe, and moreover, the magnetic excitations are relatively more important at low temperatures.

In an ordinary thermal conductivity experiment on dielectric crystals, the heat input and cooling will be through the lattice, and the thermometer readings correspond to lattice temperatures. In order to conclude whether the thermal conductivity is affected by magnetic excitations, one has to know the unaffected lattice conductivity. Furthermore a quite good interaction between the lattice vibrations and the magnetic excitations is necessary.

The possibility of thermal transport by magnetic excitations was originally suggested by Frölich and Heitler¹. Contemporary theories may be divided into three categories:

- a. thermal conductivity in magnetically ordered crystals, originally treated by Sato^{2,3,4,5}
- b. thermal conductivity in magnetically disordered (paramagnetic) crystals^{6,7,8,9}
- c. thermal conductivity near a magnetic phase transition, originally treated by Kawasaki¹⁰ and Stern¹¹.

Experimental results may be divided into the same categories:

- a. In magnetically ordered crystals, the thermal transport may partly be carried by magnetic excitations i.e. spin waves. Until recently¹³, merely the thermal conductivity of yttrium iron garnet¹² supported the idea of spin wave thermal transport. In general, it is difficult to decide whether the results in such cases are due to additional scattering of the lattice waves or to conductivity in the magnetic system.
- b. In magnetically disordered crystals, the either concentrated or diluted (para)magnetic system may have single particle excitations, such as crystalline field or Zeeman splittings. At sufficiently low temperature, the absorption and reemission of lattice waves (phonons) having an energy equal to that of the magnetic ions may be the predominant scattering mechanism. The concomittant reduction of λ may be explained as a virtual removal of a certain band of phonons from the phonon spectrum. In such systems it appears to be possible to do 'thermal spectroscopy'^{16,17,18,19}.
- c. The occurrence of an anomalous 'dip' in λ near T_N was found by Slack in MnO²⁰. The behaviour of λ near a phase transition, as reported by several authors^{21,22} may be similar to or quite different from MnO.

In the last few years some experimental and theoretical papers on the above subjects have been published, however very few problems have been solved, particularly in category c. Experimental data at very low temperatures suggest that the Debye model for the lattice vibrations is essentially correct, particularly the T^4 dependence of the phonon energy density.

However, little is known about the temperature dependence of collective excitations in a magnetic system, and virtually nothing about the corresponding transport properties. In all three categories, knowledge is lacking, both experimentally and theoretically, on the coupling of lattice vibrations to magnetic excitations below roughly 1 K. The extension of the temperature region to considerably below 1 K is desirable:

- a. to avoid complications at $T > 5$ K arising from phonon-phonon interactions and complicated interaction mechanisms between phonons and the magnetic system.
- b. since, in practice, one needs data extending over at least one decade in the temperature scale in order to derive meaningful results from the comparison with theory.

The experiments described in this thesis concern with the 'low and very low' temperature region (liquid He, and temperatures below 1 K). Experimental results in this range are commonly obtained in either a demagnetization cryostat e.g. 21,23 or an ^3He cryostat e.g. 24,25. An apparatus, similar to that described in chapter II, was reported by Harrison²⁶.

Recently measurements were reported using an ^3He - ^4He refrigerator^{15,27}.

In the following chapters we discuss primarily how to measure thermal conductivities at (very) low temperatures. Chapter I serves as an introduction to this subject and some results, obtained in a demagnetization cryostat, will be discussed. In chapter II, an apparatus to carry out thermal conductivity measurements in the range 0.05-5 K is described. Chapter III deals with temperature measurement and control in this apparatus. In chapter IV, the experimental results are presented, apart from the results on a number of magnetic crystals the thermal conductivity of He gas and its use as a thermal switch is discussed. In chapter V, the results on the conductivity in a 3D Heisenberg system, in particular near the phase transition, are compared with theories on this subject.

References

1. H. Frölich and W. Heitler, Proc. Roy. Soc. A135 (1936) 640.
2. H. Sato, Progr. Theor. Phys. Kyoto 13 (1955) 119.
3. A.I. Akhiezer, V.G. Bar'Yaktar and M.I. Kaganov, Sov. Phys. USPEKHI 3 (1961) 567, 661.
4. J.Callaway and R. Boyd, Phys. Rev. 134 (1964) 1655.
5. C.M. Bhandari and G.S. Varma, Phys. Rev. 152 (1966) 731.
6. R. Orbach e.g., Phys. Letters 3 (1963) 269.
7. R.J. Elliot and J.B. Parkinson, Proc. Phys. Soc. 92 (1967) 1024.
8. V. Roundy and D.L. Mills, Phys. Rev. B1 (1970) 370.
9. E.M. Iolin, Soviet Phys. Solid State 12 (1970) 905.
10. K. Kawasaki, Progr. Theor. Phys. 29 (1963) 801.
11. H.J. Stern, J. Phys. Chem. Solids 26 (1965) 153.
12. B. Lüthi, J. Phys. Chem. Solids 23 (1962) 35.
13. F.W. Gorter, L.J. Noordermeer, A.R. Kop and A.R. Miedema, Phys. Lett. 29A (1969) 331.
14. Chen Chou Ni, Thesis I.I.T. Chicago (1969).
15. M.J. Metcalfe and H.M. Rosenberg, Phys. Lett. 33A (1970) 211.
16. J.C.F. Brock and Huntley, Can. Journ. Phys. 46 (1968) 2231.
17. L.J. Challis, M.A. McConackie and D.J. Williams, Proc. Roy. Soc. A310 (1969) 493.
18. D. Walton, Phys. Rev. B1 (1970) 1234.
19. R.T. Harley and H.M. Rosenberg, Proc. Roy. Soc. A315 (1970) 551.
20. G.A. Slack and R. Newman, Phys. Rev. Lett. 1 (1958) 35.
21. H. van Kempen, Thesis Leiden (1965).
22. J.E. Rives, D. Walton and G.S. Dixon, Journ. Appl. Phys. 41 (1970) 1435.
23. K. Mendelsohn and C.A. Renton, Proc. Roy. Soc. A230 (1955) 157.
24. M.H. Jericho, Phil. Trans. Roy. Soc. A257 (1964) 385.
25. H. Weinstock, Phys. Letters 26A (1968) 117.
26. J.P. Harrison, Rev. Sci. Instr. 39 (1968) 145.
27. J.E. Robichaux and A.C. Anderson, Phys. Rev. B2 (1970) 5035.

CHAPTER I

INTRODUCTION TO LOW TEMPERATURE THERMAL CONDUCTIVITY

I.1 Lattice conductivity

The theory of thermal conductivity in dielectric crystals has been developed by Peierls¹. Additional material, references and discussion of experimental results may be found in review articles by several authors^{e.g. 2,3,4}. A brief review will be given here in order to provide a frame work for the discussion of experimental results.

The thermal conductivity is defined as the proportionality constant between the heat current density and the corresponding temperature gradient. In the case of a uniform rod of length L , and a cross section S one may write for the heat current

$$\dot{Q} = \frac{S}{L} \lambda \Delta T, \quad (1)$$

provided ΔT is small. In the actual experiments, eq. (1) has been used as the definition of the conductivity of a particular sample. In order to obtain the thermal conductivity, one has thus to measure the temperature difference, the heat current, and the geometry factor L/S . Theoretically, the basic problem is the calculation of the heat current, starting from the temperature gradient and certain excitations in the crystal.

In the Debye model of the solid state the excitations in a dielectric crystal are lattice waves, or phonons, having wave vector k and frequency ω . Usually the phonon velocity, i.e. the group velocity $\frac{d\omega}{dk}$, is taken as a constant (v). Though it is not used explicitly, we assume for simplicity the crystal to be an isotropic monatomic lattice.

Consider the flow of phonons through the walls of a small volume in which neither the number of phonons nor their energy are separately conserved. The number of phonons within this volume, e.g. those of a particular wave vector n_k , changes for two reasons:

- a. collisions of phonons, with each other and with impurities. This may be written as $\frac{\partial n_k}{\partial t}$, and must be calculated according to the detailed scattering mechanisms involved.
- b. transport of phonons due to a temperature gradient. This may be expressed by

$$-v_k \cdot \text{grad} n_k \text{ or } -v_k \cdot \text{grad} T \frac{\partial n_k}{\partial T}.$$

In the steady state the total rate of change must be zero (continuity equation for the phonons), so we arrive at the Boltzmann equation

$$\frac{\partial n_k}{\partial t} = \mathbf{v}_k \cdot \text{grad} T \frac{\partial n_k}{\partial T}. \quad (2)$$

In general eq. (2) is a complicated integral equation. An important simplification may be made by the relaxation time assumption

$$\frac{\partial n_k}{\partial t} = -\frac{n_k}{\tau_k}. \quad (3)$$

This assumption appears to give a good approximation in practice^{4,5}. The relaxation time assumption is especially useful if it is also assumed that scattering processes are mutually independent; and the combined relaxation time is given as⁴

$$\frac{1}{\tau_k} = \sum_i \frac{1}{\tau_{ki}}. \quad (4)$$

This assumption is analogous to Matthiesen's rule in the theory of metals.

The heat current may be expressed as

$$\dot{Q} = \sum_k n_k \hbar \omega_k \mathbf{v}_k \cos \varphi_k, \quad (5)$$

where φ_k is the angle between \mathbf{v}_k and $\text{grad} T$.

Combination of eq. (2), (3) and (5) leads to

$$\dot{Q} = \sum_k \frac{\partial n_k}{\partial T} \hbar \omega_k v^2 \tau_k \Delta T, \quad (6)$$

where v^2 is an average of $v_k^2 \cos^2 \varphi_k$.

The internal energy is given by $n_k \hbar \omega_k$ and thus the specific heat $c_k = \hbar \omega_k \frac{\partial n_k}{\partial T}$. Substituting this into eq. (6) and combining with eq. (1) leads to

$$\lambda = \sum_k c_k v^2 \tau_k = \sum_k c_k v l_k, \quad (7)$$

which is analogous to the kinetic gas theory formula. To arrive at the familiar formula for the thermal conductivity in the Debye model we use:

- The density of states in k space is sufficiently great that the summation over k may be replaced by an integral.
- Normally the integral has an upper limit at a certain maximum k value (defining the Debye temperature θ_D). However, for $T \ll \theta_D$ the exponential dependence of c_k

$$c_k(\omega) \sim \frac{(\hbar \omega)^2}{k_B T^2} \frac{e^{\hbar \omega / k_B T}}{(e^{\hbar \omega / k_B T} - 1)^2}, \quad \text{allows us to set the upper bound equal to } \infty.$$

c. It is convenient to change to the dimensionless variable $x = \hbar\omega/k_B T$.

Combining a, b, and c, with eq. (7) leads to

$$\lambda = \frac{v^2 k_B}{2\pi^2} \left(\frac{k_B T}{\hbar v} \right)^3 \int_0^\infty x^2 \tau_k(x) c_k(x) dx \quad (8)$$

Consider the idealized case $\tau_k \sim k^{-n} = \frac{k_B T}{\hbar v}^{-n} x^{-n}$, then eq. (8) becomes

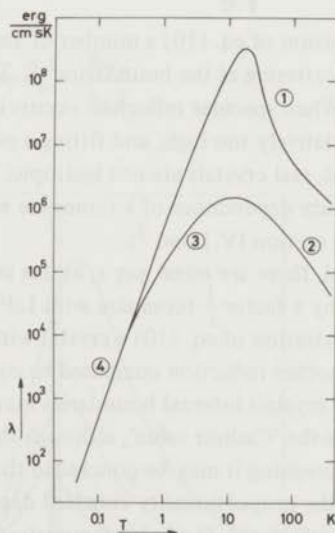
$$\lambda \sim T^{3-n} \int_0^\infty \frac{x^{4-n} e^{-x}}{(e^x - 1)^2} dx \sim T^{3-n}, \quad (9)$$

which is a useful rule for finding the temperature dependence of λ in a particular scattering process. In this way, the most important scattering processes in dielectric crystals give rise to characteristic temperature dependences of λ (see fig. 1):

- | | |
|-----------------------------|--|
| 1. phonon-phonon scattering | $\lambda \sim T^3 e^{\frac{\theta_D}{aT}}$ |
| 2. point-defect scattering | $\lambda \sim T^{-1}$ |
| 3. dislocation scattering | $\lambda \sim T^2$ |
| 4. boundary scattering | $\lambda \sim T^3$ |

Fig. 1.1

Thermal conductivity as a function of temperature, the numbers refer to different scattering processes.



Since usually a combination of these scattering processes are simultaneously operative, it is difficult to say which T dependence is expected. But if T is low enough, the conductivity will be limited by boundary scattering alone, and λ varies as T^3 ; this was originally derived by Casimir⁶ using a theory analogous to black body radiation.

As already stated in the introduction, the study of spin-phonon interaction is best performed at low temperatures. At this stage this statement can be made more precise as far as the phonons are concerned. Low temperatures are preferred because:

- Only boundary scattering is important, the other 'intrinsic' phonon processes being frozen out.
- The T^3 dependence for λ means a maximum lattice conductivity, hence λ is as sensitive as possible for other, e.g. magnetic, phonon scattering processes.
- λ is independent of point defects, so chemical purity is not very important, hence the requirements for the crystals are not difficult to meet. The reverse may be true in studies on the phonon scattering by dilute magnetic impurities; however, this thesis pertains to the study of magnetically concentrated crystals.

The ' T^3 conductivity' may be calculated from eq. (8) as

$$\lambda = 6.47 \times 10^7 \frac{\rho v}{M \theta_D^3} T^3 \text{ erg/cm s K}, \quad (10)$$

where ρ is the crystal density and M is the molecular weight.

Either v or θ_D may then be eliminated, using the relation

$$\theta_D = 2.52 \times 10^{-3} v \sqrt[3]{\frac{\rho}{M}}. \quad (11)$$

In the derivation of eq. (10) a number of assumptions were made:

- Diffuse scattering at the boundaries^{3,6}. This assumption may be invalid for long wavelengths. When specular reflection occurs instead of diffuse scattering, the conductivity will be relatively too high, and fitting a power law $\lambda \sim T^n$ to the data, $n < 3$ will be found.
 - In general, real crystals are not isotropic. Elastic anisotropy does not affect the temperature dependence of λ (compare with the discussion on the thermal conductivity of LiF in section IV.1 and ⁷).
 - In general, there are more, say s , atoms in a unit cell, this means that one has to reduce eq. (10) by a factor $\frac{1}{s}$ (compare with LiF in section IV.1).
 - In the derivation of eq. (10) a crystal with infinite length is assumed. The finite length causes another reduction compared to eq. (10)^{3,8}.
 - In actual crystals internal boundaries may occur, in which case the mean free path will not reach the 'Casimir value', although the conductivity may remain proportional to T^3 .
- From the foregoing it may be concluded that a T^3 dependence at low temperatures is quite likely, but the proportionality constant depends on so many factors that it can not, in general, be calculated. It can be demonstrated⁹ that if the maximum in λ is reached at, say T_M , the T^3 dependence will almost certainly be realized for $T < T_M/10$, independently of the dominant scattering processes at higher temperatures. For hydrated crystals T_M will usually be found between 5 K and 15 K, hence a T^3 dependence of λ is expected for temperatures lower than 1 K.

I.2 A simple model for phonon scattering in a magnetic crystal

In the preceding section we concluded, from the phonon point of view, that low temperatures are preferred for studying the interaction between the lattice and magnetic excitations by means of thermal conductivity measurements. Now we will investigate which kind of behaviour we can expect for λ in the presence of magnetic excitations, beginning with the following simplifying assumptions:

- The temperature at which λ is measured is such that boundary scattering is the only intrinsic process.
- The magnetic system is described by an energy splitting $\hbar\omega_0$ and a bandwidth $\hbar\Delta\omega$ (for instance a spin $\frac{1}{2}$ paramagnet in a magnetic field H).
- Phonons having frequencies between $\omega_0 - \frac{\Delta\omega}{2}$ and $\omega_0 + \frac{\Delta\omega}{2}$ are scattered so strongly that they no longer contribute to the thermal transport.

Without magnetic scattering, the conductivity is

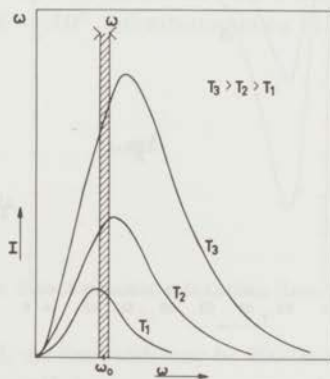
$$\lambda = AT^3 \int_0^{\infty} I(x) dx, \text{ with } I(x) = \frac{x^4 e^x}{(e^x - 1)^2} \quad (12)$$

Due to the magnetic system, λ will change and, as a consequence of c, this change, $\Delta\lambda$, will be given as (see fig. I.2)

$$\Delta\lambda = AT^3 \int_{x_0 - \frac{\Delta x}{2}}^{x_0 + \frac{\Delta x}{2}} I(x) dx \approx AT^3 I(x_0) \Delta x, \text{ where } x_0 = \frac{\hbar\omega_0}{k_B T} \quad (13)$$

Fig. I.2

Phonon distribution at different temperatures.
According to the assumptions for the band model, phonons having frequencies within the band, centered at ω_0 , do not contribute to the thermal transport.



Usually experimental results are presented as $\frac{\Delta\lambda}{\lambda} = \frac{\lambda(H) - \lambda(0)}{\lambda(0)}$ versus H or $\frac{\hbar\omega_0}{k_B T}$, and $\frac{\Delta\lambda}{\lambda}$ may be expressed by $\frac{\Delta\lambda}{\lambda} = -CI(x_0)\Delta x = CI(x_0)\frac{\hbar\Delta\omega}{k_B T}$ (14)

Here we meet another advantage of measuring these effects at low temperatures: the effect, inversely proportional to T , becomes more important at lower temperatures.

In principle, there are two ways to measure this magnetic scattering:

- a. Constant magnetic field and variable temperature method. At constant ω_0 and variable T , the scattering will be largest for maximal $I(x_0)/T$, i.e. for $T \approx \hbar\omega_0/5k_B$ (see fig. I.3) and the magnitude of the scattering will be

$$\frac{\Delta\lambda}{\lambda} = 0.73 \frac{\Delta\omega}{\omega_0} \quad (14a)$$

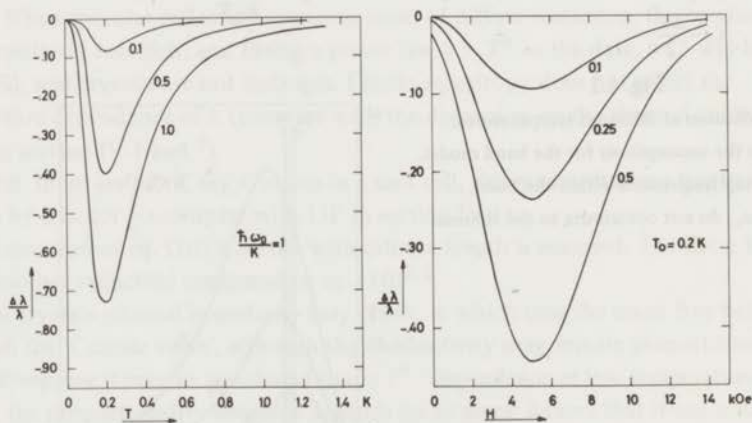
- b. Constant temperature and variable field method. At constant T and variable ω_0 (that is variable magnetic field strength), the scattering is largest for maximal $I(x_0)$, i.e. for $H \approx 4k_B T/g\mu$ (see fig. I.3), and the magnitude of the scattering will be

$$\frac{\Delta\lambda}{\lambda} = 0.188 \frac{\hbar\Delta\omega}{k_B T_0} \quad (14b)$$

Concluding, one may say that the height of the scattering maximum is proportional to the phonon-spin interaction bandwidth, and, in this simple 'band-model', the form of the curve is entirely determined by the phonon spectrum.

Fig. I.3

Computed change in λ for the band-model, the curves are labelled with their bandwidth in K.



Experimental data concerning phonon-spin interaction strengths are scarce; on the other hand, many spin-phonon interaction data (paramagnetic relaxation) are known. It is therefore interesting to relate the mean free path ($\nu\tau$) of the scattered phonons with the spin-

lattice relaxation time. The assumptions b and c correspond to the so called direct process considered in the theory of spin lattice relaxation. Although we encounter here the important question of the line shape¹⁰ it is simply assumed, as in the preceding discussion, that all phonons within the band interact 'quite strongly' with the magnetic system, while phonons outside the band have no interaction with the magnetic system (compare with¹¹).

The phonon relaxation time τ is given by the ratio

$$\tau = \frac{\text{total number of phonons in band}}{\text{total number of absorbed phonons per second}} \quad (15)$$

The spin-phonon relaxation time T_1 is related to the transition probability, W , according to¹²

$$T_1 = \frac{1}{W} \operatorname{tgh} \frac{\hbar\omega_0}{2k_B T}, \quad (16)$$

eq. (15) may be expressed in the phonon density of states ρ and the population density p of the phonon and spin system as

$$\tau = \frac{\rho(\hbar\omega_0)p(\hbar\omega_0)\hbar\Delta\omega}{W(N_a - N_b)p(\hbar\omega_0)}. \quad (17)$$

Substitution of the relevant quantities in eq. (17) leads to

$$\tau = \frac{3\hbar^2\omega_0^2\hbar\Delta\omega}{2\pi^2v^3\hbar^3WN} \operatorname{coth} \frac{\hbar\omega_0}{2k_B T}, \quad (18)$$

where N is the number of spins per unit volume.

Now suppose the magnetic energy splitting to be caused by an external field, so that $\hbar\omega_0 = g\mu H$; the bandwidth expressed in magnetic field units is ΔB , and it can be shown for a direct process in a Kramers doublet¹³ that $W = AH^5$. Substitution in eq. (18) gives rise to

$$\tau = \frac{3g^3\mu^3\Delta B}{2\pi^2v^3\hbar^3NA} H^{-3} \operatorname{coth} \frac{g\mu H}{k_B T}, \quad (19)$$

which may be evaluated to

$$\tau = 10^{-18} \frac{\Delta B}{A} H^{-3} \operatorname{coth} \frac{g\mu H}{k_B T}. \quad (20)$$

A may be found with the aid of eq. (16) if the direct process relaxation time is known from experiments.

For instance, in a typical paramagnetic crystal, the linewidth may be 200 Oe and the relaxation time $0.2 T^{-1}$ s, implying $W \approx 1$ and $A \approx 10^{-15}$. In the case of interest, the coth is about 1, thus $\tau = 0.2 H^{-3}$ s. From these numbers we conclude that the assumption c (phonons within the band do not contribute to the thermal transport) is fulfilled if $H > 1000$ Oe.

I.3 Experimental requirements

Suppose the experiment aims at an accuracy of 1% in the thermal conductivity λ . Then a number of experimental requirements can be formulated.

a. Sensitivity of the thermometry.

It should be realized that $\dot{Q} = \lambda \Delta T$ is an approximation of the integral equation (21)

$$\dot{Q} = \int_T^{T+\Delta T} \lambda dT. \quad (22)$$

In order to evaluate this approximation, we consider the case $\lambda = AT^n$; then one finds with eq. (22)

$$\dot{Q} = AT^n \Delta T \left(1 + \frac{n}{2} \frac{\Delta T}{T} + \dots \right). \quad (23)$$

Hence not only ΔT , T and \dot{Q} need to be known with an accuracy of better than 1% but also $\Delta T/T$ itself should be 1/n % in order to be able to apply eq. (21) instead of eq. (23).

So the temperature sensitivity has to be better than 1/n parts in 10^4 .

b. The heat leak.

In general, the conductivity of the samples is of the order of magnitude of $10^5 T^3$ erg/s K. So, for example at $T = 0.1$ K, the maximum heat current through the sample will be about 0.03 erg/s. In order to measure λ , the heat leak has to be considerably smaller.

c. Dimensions of the sample.

At low temperatures, the wavelength of the phonons becomes very long, on the other hand the mean free path will be of the order of magnitude of the crystal diameter. It is evident, that the theory, outlined in section I.1, may merely be used if the dominant phonon wavelength is much smaller than the crystal diameter. The dominant phonon wavelength can be estimated with

$$\frac{\theta_D}{T} \times \text{lattice spacing.}$$

Taking a lattice spacing of 5 \AA and $\theta_D = 60$ K, the dominant wavelengths will be approximately $300/T \text{ \AA}$, which is negligible compared to the actual sample diameters, even at the lowest temperatures. However, for instance in diamond ($\theta_D = 2000$ K), the wavelengths may be as large as 0.01 mm, and it becomes doubtful whether the simple phonon concept is applicable in this temperature range.

I.4 Method for measuring thermal conductivity below 1 Kelvin

Temperatures below 1 K are easily obtained by adiabatic demagnetization. Van Kempen¹⁴ reported a method for measuring λ below 1 K. That method with two magnetic thermometers, shows disadvantages due to the problem of the calibration accuracy of a magnetic

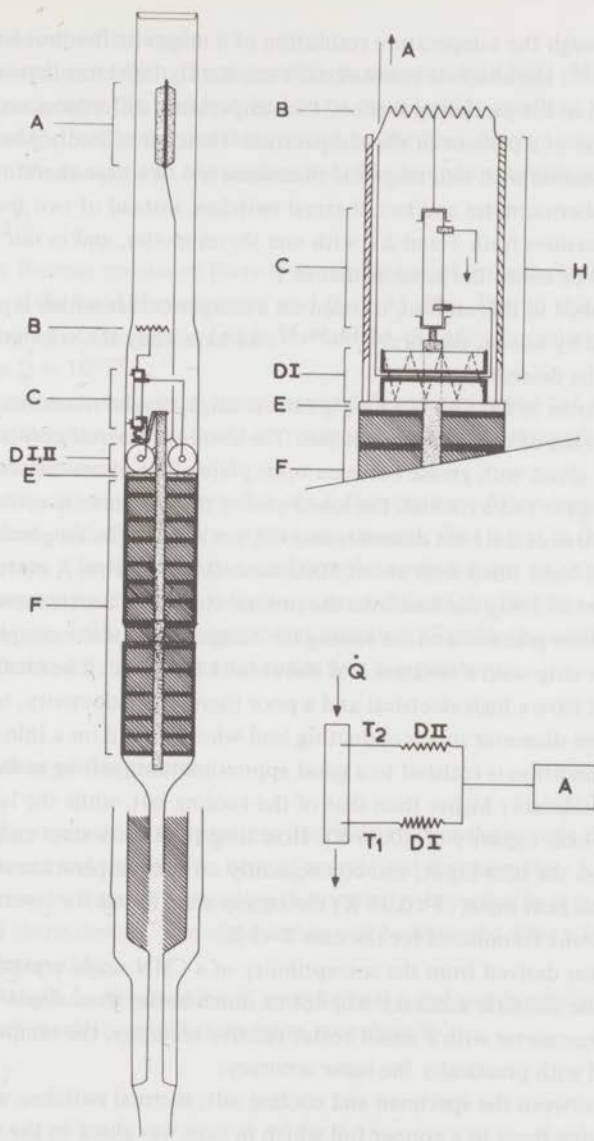


Fig. I.4

Apparatus for measuring thermal conductivity below 1 K.

A: magnetic thermometer; B: heater; C: specimen; D_I, D_{II}: coils and thermal switches; E: perspex insulating plate; F: cooling salt; H: connection to heater (lead wires on nylon).

thermometer. Although the temperature resolution of a magnetic thermometer may be about 1 part in 10^4 ¹⁵, the absolute measurement can hardly be better than a few tenths of a percent. As stated in the preceding section, the temperature differences are also in the order of a few tenths of a percent of the temperature. Hence it is hardly possible to make accurate λ measurements with two magnetic thermometers. We have therefore chosen a method using one thermometer and two thermal switches, instead of two thermometers. In this way, one measures both T and ΔT with one thermometer, and in our case the accuracy in ΔT will be about the same as that in T .

The method, described in this section, is based on a sample-holder which is part of an apparatus described by several authors^{e.g. 14, 16, 17}. So here, only the relevant part of the sample-holder will be described.

The apparatus is shown in fig. I.4. The Ce-Mg-nitrate single crystal measures the two temperatures by means of the thermal switches. The cooling reservoir consists of Cr-K-alum single crystal slabs, glued with grease between brass plates. The plates are screwed to a 0.3 cm diameter copper rod by which the lower end of the specimen is cooled. The thermal switches are lead wires of 0.01 cm diameter and 0.5 cm length. The (superconducting) lead is inside a brass coil form filled with about 5000 turns 0.05 Nb wire. A current of about 200 mA is sufficient to bring the lead into the normal state. The heater serves both for creating a temperature gradient and for raising the temperature of the sample as a whole. As a heater, a brass strip with a resistance of about 0.01 Ω is used. Electrical contact to the heater, which must have a high electrical and a poor thermal conductivity, is provided by 15 cm long, 0.01 cm diameter superconducting lead wires, wound on a thin nylon rod. The steady state condition is realized to a good approximation, as long as the sample temperature is considerably higher than that of the cooling salt, while the latter has to be in the region of large heat capacity ($T < 0.25$ K). How long the steady state can be maintained depends strongly on the heat input, and consequently on the temperature at which λ is measured. For small heat input ($T < 0.25$ K) the steady state lasted for several hours, whereas this time is only about 10 minutes for the case $T \approx 1$ K.

The temperature was derived from the susceptibility of a CMN single crystal thermometer. As stated earlier, the absolute accuracy will not be much better than about 1%; but since we used only one thermometer with a much better relative accuracy, the temperature gradient could be measured with practically the same accuracy.

Thermal contact between the specimen and cooling salt, thermal switches, and heater, was obtained by soldering them to a copper foil which in turn was glued to the specimen with Apiezon N grease. The samples were cut from large single crystals, abraded to suitable dimensions (about $\frac{1}{4} \times \frac{1}{4} \times 2$ cm), and selected in such a way that they were optically transparent.

In fig. I.4, the switches are shown mounted on the top of the cooling salt. A slightly different version, in which the switches were mounted between the sample and the thermometer, was also used. The latter has the advantage of easier sample mounting but is less

compact compared to the first version.

With the above precautions taken, it was possible to measure with heat currents as low as 0.1 erg/s, and consequently the heat leak had to be considerably smaller.

The temperature of the 'cold side' was determined by the heat current and the boundary resistance between the sample and the cooling rod. The boundary resistance can be given as¹⁷

$$\dot{Q} = 10^5 S(T_1^4 - T_2^4).$$

In addition to this thermal resistance there is the resistance of the sample itself (between the connection point of the 'cold thermometer' and the cold side). Due to this resistance and the nonideal mounting of the copper foil to the sample, the effective relation between T and \dot{Q} was found to be $\dot{Q} = 10^3 T^4$.

This thermal resistance caused a large temperature difference between the sample and the cooling rod. Hence the steady state could be realized although the temperature of the cooling salt rose continuously.

The actual measurements were performed in the following way. After demagnetization a certain \dot{Q} was applied, and one of the switches was opened, that is put in the normal, i.e. heat conducting, state. The thermometer (and sample) cooled down to an equilibrium temperature. Subsequently the other switch was opened (and the first one closed), and the temperature of the other side of the sample was measured. Finally the attainment of the steady state was checked by measuring again the first temperature.

1.5 Equilibrium time of the process

The attainment of a stationary temperature distribution over the sample depends on the particular heat current and the specific heat of sample and thermometer. A characteristic time constant, τ , may be found by assuming that initially the entire heat current is absorbed by the sample and thermometer. The steady state will be obtained after a few times this characteristic time constant.

Take a sample of length L , cross section S , specific heat c and conductivity λ . The temperature difference will reach its equilibrium value according to

$$\frac{S}{L} \lambda \Delta T = -LSc \frac{d\Delta T}{dt}, \quad (24)$$

having the characteristic time $\tau = L^2 c / \lambda$ which may be considered as a reasonable estimate for the time constant. (25)

The conductivity at low T is given by

$$\lambda = \frac{1}{3} cvl. \quad (26)$$

Inserting eq. (26) into eq. (25), τ appears to be temperature independent and taking for

instance $L = 1$ and $l = 0.1$ we find τ to be about 10^{-4} s.

For a paramagnetic crystal, the specific heat may be expressed by

$$c = \frac{a}{T^2} + bT^3. \quad (27)$$

Substitution of eq. (26) and eq. (27) in eq. (25) leads to

$$\tau = \frac{3L^2}{\nu l} \left(\frac{a}{b} T^{-5} + 1 \right). \quad (28)$$

This characteristic time becomes very long at low temperatures, e.g. the alums ($\frac{a}{b} \approx 35$) give rise to $\tau = 3 \times 10^{-3} T^{-5}$ s, hence $\tau = 300$ s at 0.1 K. The time required to obtain the steady state is considerably (5-10 times) longer.

For the thermometer with a specific heat of $2T^{-2}$ erg/K and $\frac{a}{b} = 0.5$, a similar estimate may be made, leading to $\tau = 10^{-4} T^{-5}$ s. After operating the thermal switches, the thermometer has to cool down (warm up), which corresponds to a removal of $c\Delta T$ erg. Inserting the values for CMN this amounts to $2 \times 10^{-2} T^{-1}$ erg. At low temperatures, the removal of this thermal energy seriously distorts the steady state, since the corresponding heat flow is of the same order of magnitude as the heat current $\lambda\Delta T$ which was already present.

The conclusion of this discussion is, that the time needed for steady state measurements at low temperatures, becomes very long indeed.

1.6 Some experimental results

LiF, a diamagnetic crystal

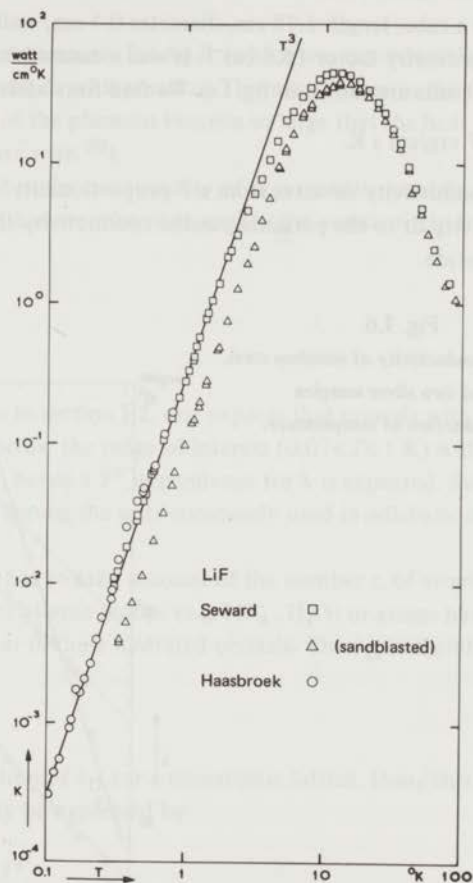
LiF is a cubic crystal with a high Debye temperature (722 K), and has therefore been used in a number of experiments to study lattice conductivity. The sample was grown at the Harshaw Chemical Company, its thermal conductivity was measured by Seward and Thacher at Cornell University, and it was kindly given to us by professor R.O. Pohl.

As a consequence of the high Debye temperature one may expect the thermal conductivity to be proportional to T^3 over the whole temperature range of interest. Therefore this LiF sample serves as a check of the method. Unfortunately the crystal was too large (dimensions 0.55 x 0.52 x 4.1 cm) to measure in the mentioned version of the apparatus, while it was undesirable to change the sample shape. Hence the results shown in fig. I.5 were obtained in the second, enlarged version of the apparatus.

The agreement with the measurements of Seward is satisfactory, and the conductivity is indeed proportional to T^3 . A detailed discussion of the thermal conductivity of LiF will be given in section IV.1.

Fig. I.5

Thermal conductivity of LiF as a function of temperature.



Metals

In order to measure metals with our 'switch apparatus', one has to make electrically insulated contacts, since otherwise the use of the switches would cause a considerable heat input.

In metals, the heat transport will be due to both electrons and phonons. Hence $\lambda = \lambda_e + \lambda_p$. In the low temperature limit and using the kinetic formula $\lambda = \frac{1}{3}c\bar{v}l$ one can show λ_e to be proportional to T and λ_p to be proportional to T^2 (see e.g. 18). In general, λ_p will be negligible in pure metals; but in alloys, in a certain temperature range, λ_p may be an appreciable part of the conductivity.

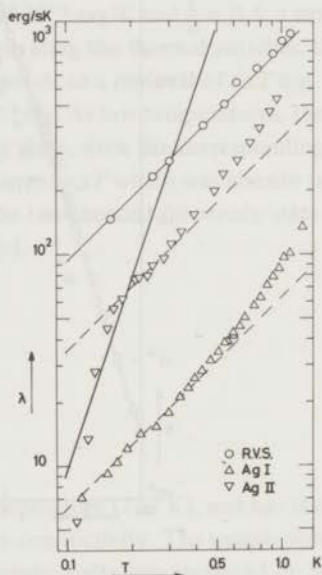
Stainless steel

The sample was a tube, length 2.78 cm, diameter 0.4 cm, wall thickness 0.05 cm, and mounted with geometry factor 15.8 cm^{-1} . It was measured in the enlarged version of the apparatus; the results are shown in fig. I.6. We find for stainless steel at low temperatures

$$\lambda = 1.45 \times 10^4 T \text{ erg/cm s K.}$$

Near 1 K the conductivity deviates from a T proportionality. Whether this is due to the lattice conductivity or to the parasitic parallel conductivity through the switches (see fig. I.4) is difficult to decide.

Fig. I.6
Thermal conductivity of stainless steel,
and two silver samples
as a function of temperature.



Silver

The silver sample Ag I (dimensions about $10 \times 0.1 \times 0.01 \text{ cm}$) was of high purity Ag. Ag II was $\frac{1}{5}$ of the length of Ag I. Sample Ag II was also measured in the range 1.3 - 4 K*, the conductivity being linear and given by

$$\lambda = 353 T \text{ erg/s K.}$$

As can be seen in fig. I.6 this value fits to the measurements between 0.2 and 0.3 K. The parallel conductivity through the switches is expected to show a T^3 dependence¹⁹. Therefore the results were fitted to the formula $\lambda = aT + bT^3$. Although this formula gives

* We thank dr. W.M. Star for doing the measurement for us.

a fair description of the data, the fact that the coefficient b varies with the length of the sample is not understood.

The steep descent of λ at low temperatures for Ag II (which was reproducible in different series on the same and on different days) is peculiar. This may be due to the fact that the mean free path and wavelength of the phonons become so large that the heat transfer to the sample may be impeded (compare with ²⁰).

Since we are primarily interested in the conductivity of non-metallic crystals, we shall not go into details, but merely state that even for pure metals, the conductivity is not as simple as expected.

Paramagnetic crystals

In view of the band-model, given in section I.2, one expects that crystals with splittings corresponding to temperatures below the range of interest ($0.07 < T < 1$ K) will show an undisturbed lattice conductivity, hence a T^3 dependence for λ is expected. Such paramagnetic crystals may be found among the salts commonly used in adiabatic demagnetization experiments.

As was stated in section I.1, one has to take account of the number s , of atoms in the unit cell. Since it is uncertain, whether atomic groups (e.g. NH_4 , H_2O) or atoms have to be counted, the value of s is not clear in these hydrated crystals. The θ_D is therefore, at very low T , usually defined by

$$c_{\text{mol}} = 1941 \left(\frac{T}{\theta_D} \right)^3 \text{ J/mol}, \quad (29)$$

thus corresponding to the definition of θ_D for a monatomic lattice. Using this definition of θ_D , the thermal conductivity may be expressed by

$$\lambda = 2.57 \times 10^{12} \frac{1}{s} \sqrt[3]{\frac{\rho^2}{M^2}} \frac{1}{\theta_D^2} l T^3, \quad (30)$$

where l should correspond to the sample diameter. In the following analysis we have taken the number of atomic groups for the value of s , hence for instance for the alums $s = 16$ (compare with ²⁷).

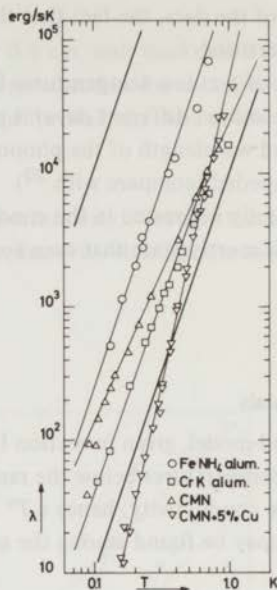
FeNH₄-alum (dimensions: 2.7 x 0.34 x 0.34 cm, geometry factor: 9.1 cm⁻¹)

The conductivity is shown in fig. I.7, and for $T < 0.4$ K it was found to be

$$\lambda = 2.3 \times 10^6 T^3 \text{ erg/s cm K.}$$

Substitution of this experimental value for λ , $\theta_D = 82.3 \text{ K}^{2/3}$, $\rho = 1.71$, and $M = 482$ in eq. (30) yields a mean free path of 14 times the crystal diameter. From this value, we may conclude that specular reflection of the phonons at the crystal boundaries occurs.

Fig. I.7
Thermal conductivity
of four dielectric, hydrated, paramagnetic crystals
as a function of temperature.



CrK-alum (dimensions: $4 \times 0.35 \times 0.33$ cm, geometry factor: 8.5 cm^{-1})

The conductivity is shown in fig. I.7, and for $T < 0.25$ K it was found to be

$$\lambda = 3.3 \times 10^5 T^3 \text{ erg/s cm K.}$$

Taking $\theta_D = 77.9$ K, $\rho = 1.83$, and $M = 499$, eq. (30) yields a mean free path of 1.6 times the sample diameter, so that we find in this case a fair agreement between our experimental result and the Debye theory. Moreover, the absolute value agrees quite well with that reported by Van Kempen¹⁴ and Garret²².

CeMg-nitrate (dimensions: $1.8 \times 0.33 \times 0.31$ cm, geometry factor: 5.0 cm^{-1})

Several samples of CMN are measured, both the absolute value and temperature dependence ($\sim T^n$ with $2.5 < n < 3$) depended on the particular sample. This must be due to lattice defects (compare with section IV.3). For comparison with the following sample, one of the results on CMN is shown in fig. I.7; this conductivity corresponds to a mean free path of about 7 times the crystal diameter.

CeMg-nitrate with 5% Cu (dimensions: $2.1 \times 0.39 \times 0.30$ cm, geometry factor: 5.5 cm^{-1})

In this sample, 5% of the Mg are replaced by Cu. The remarkable fact in this case is that the temperature dependence (λ proportional to $T^{4.5}$) is very different from that in pure CMN (see fig. I.7). Since such a high power of T cannot be caused by an intrinsic phonon process,

it has to be due to phonon scattering by the Cu ions.

Similar temperature dependences were reported for the thermal conductivity of KMgF_3 in which a part of the Mg was replaced by Ni^{23} .

Linear chain crystals

In magnetic crystals, in addition to the intrinsic phonon processes, phonon scattering by the magnetic system may occur. On the other hand diffusion or wave-like excitations ('spin-waves') in the magnetic system may give rise to an additional heat transport. Since, in general, the phonon conductivity in itself is a quantity which is not known, it is difficult to make a distinction between the two effects.

There are a number of magnetic crystals in which the magnetic exchange coupling is predominantly among ions lying along a certain direction of the crystal, for instance along a crystallographic axis, thus forming a magnetic linear chain. Heat transport in the magnetic system, if any, should merely occur in the direction of this chain. Hence, measuring the conductivity in such a crystal perpendicular to and parallel to the chain, the two effects may be separated: in the first case only scattering occurs and in the second both scattering and additional transport may be found. We therefore measured the conductivity of two 'chain crystals' in different directions. The results above 1.5 K were obtained by dr. F.W. Gorter.

$\text{Cu}(\text{NH}_3)_4\text{SO}_4 \cdot \text{H}_2\text{O}$

It was shown (e.g. ²⁴) that copper-tetraamine-sulfate behaves like a one-dimensional Heisenberg antiferromagnet, in which the chains lie along the *c* axis. At $T_N = 0.37$ K, three-dimensional long range order occurs throughout the crystal, due to interaction between the chains.

The samples were cut from different single crystals*. The results of the heat conductivity measurements are shown in fig. 1.8. Two other samples, cut perpendicular to the *c* axis, were also measured and the results agreed with fig. 1.8 at least in as much as the temperature dependence is concerned ($T > 0.3$ K, $\lambda \sim T^2$ and $T < 0.3$ K, $\lambda \sim T^3$).

The difference in temperature dependence between the results for the perpendicular direction ($\lambda \sim T^2$) and those for the parallel direction ($\lambda \sim T^{2.5}$) is attributed to the magnetic system. An analysis of this result obtains as follows.

Let us define:

l is the mean free path associated with boundary scattering (which is found for $T < 0.3$ K)

l_m is the mean free path under influence of the magnetic system

l_e is the effective mean free path derived from the measurements

l_e can be given by

$$l_e^{-1} = l^{-1} + l_m^{-1}.$$

* kindly placed to our disposal by prof. Haseda.

Fig. I.8

Thermal conductivity of copper tetraamine sulfate; the heat flow being either perpendicular to or parallel to the magnetic linear chain i.e. c axis.

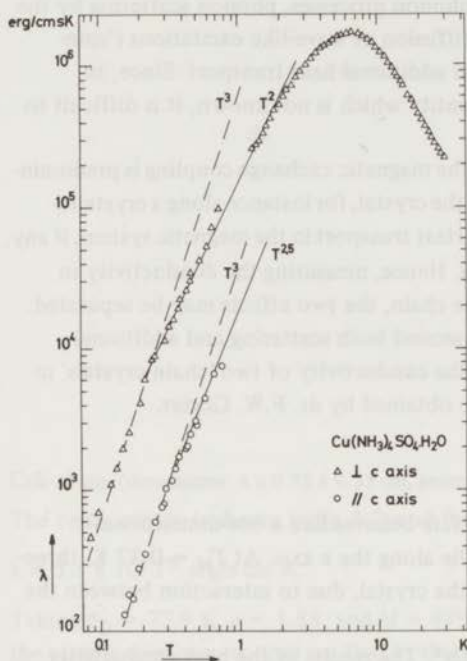
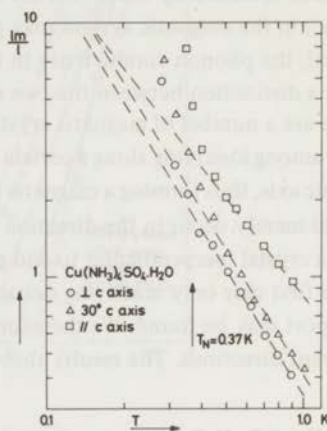


Fig. I.9

Mean free path for magnetic scattering in a linear chain crystal; the heat flow being either perpendicular to, or parallel to, or making 30° with the magnetic linear chain i.e. c axis.



The quantity l_m/l (which shows the effect of the magnetic system) may be expressed in measured conductivities as

$$\frac{l_m}{l} = \left(\frac{\lambda_o}{\lambda} - 1 \right)^{-1}$$

in which λ_o is the T^3 conductivity. In fig. I.9 l_m/l versus T is shown, and we notice that:

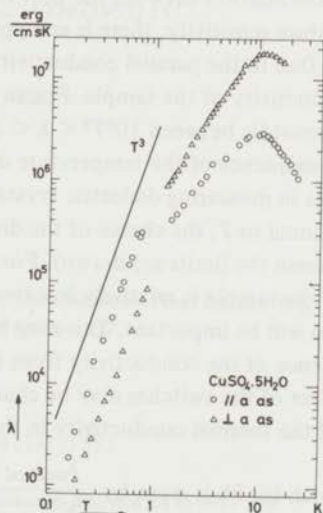
- The temperature dependence of l_m/l for $T > 0.5$ K is the same for the samples with longest direction perpendicular to or making 30° with the c axis. However, it is different for the sample cut parallel to the c axis. This strongly suggests that the difference is not due to anisotropic spin lattice interaction or to anisotropy in the lattice conductivity, but a consequence of transport in the magnetic linear chain.
- The onset of long range order is seen as a change in temperature dependence of l_m/l .

$\text{CuSO}_4 \cdot 5\text{H}_2\text{O}$

Miedema e.a.²⁵ suggested that in this substance, one half of the Cu ions are magnetically coupled in antiferromagnetic linear chains, whereas the remaining Cu ions are very weakly coupled, i.e. showing paramagnetic behaviour down to ≈ 0.05 K. Further Wittekoek e.a.²⁶ investigated this compound by proton N.M.R., in order to identify at which crystallographic positions the Cu ions, which took part in the intra chain coupling, were located. The direction of the chain is found in our conductivity measurements to be along the a axis (fig. I.10).

Fig. I.10

Thermal conductivity of copper sulfate;
the heat flow being either perpendicular to or parallel to
the magnetic linear chain i.e. a axis.



The results shown in fig. I.10 have been obtained from 4 samples cut from the same single crystal. The conductivity appears to be very anisotropic (a factor of about 5 between parallel and perpendicular direction). This was further checked by measuring the temperature gradient perpendicular to the heat flow for a sample having its longest direction making 45° with the a axis.

Unfortunately there is not a definite indication of the T^3 dependent conductivity; so we can not make the same analysis as was made for copper-tetraamine-sulfate.

Neither the experiments nor the theoretical discussions of the mentioned thermal conductivities are complete. However, some general conclusions may be drawn:

- Magnetic effects in thermal conductivity may indeed occur in a wide temperature range.
- Thermal transport by the magnetic excitations may be as large as that by the lattice, even if only short range magnetic order exists.

1.7 Discussion of the method

The results, mentioned in the preceding section, especially those with LiF and stainless steel, confirm the expectation that it is possible to measure λ with our 'switch apparatus'. The results on the hydrated salts confirm the conclusion of Van Kempen¹⁴ that, although these samples have been repeatedly cooled and recycled to room temperature, they do reproduce in general.

There are a number of difficulties encountered in this method, namely:

- a. Due to the relation between the heat flow, the mean temperature of the sample, and the temperature sensitivity, there is an upper bound for the admissible conductivity of the sample. Due to the parallel conductivity through the switches there is a lower bound for the conductivity of the sample. For an accurate measurement the conductivity of a sample must lie between $10^4 T^3 < \lambda < 3 \times 10^6 T^3$ erg/s K.
As a consequence of the temperature dependence, these limits will not give serious problems in measuring dielectric crystals. However, for metal samples, with a conductivity proportional to T , the choice of the dimensions becomes very important (compare fig. I.6, I.7, wherein the limits are drawn). For instance in the measurement of Ag, the conductivity of the sample is relatively low near 1 K, hence the parallel conductivity through the switches will be important. This may be the origin of the deviation from a linear T dependence of the conductivity from these samples.
- b. The effect of the switches may be characterized by a switch factor which is defined as the ratio of the thermal conductivity in the normal state to that in the superconducting state,

and which for Pb is given by
$$\frac{\lambda_{\text{normal}}}{\lambda_{\text{supercond.}}} = 45 T^{-2}.$$

Thus 1 K presents an upper limit for the switch method. Due to the equilibrium times at low temperatures (section I.5), there is an effective low temperature limit, which depends slightly on the particular sample. For an accurate measurement of λ the temperature is limited to the range $0.07 < T < 1$ K.

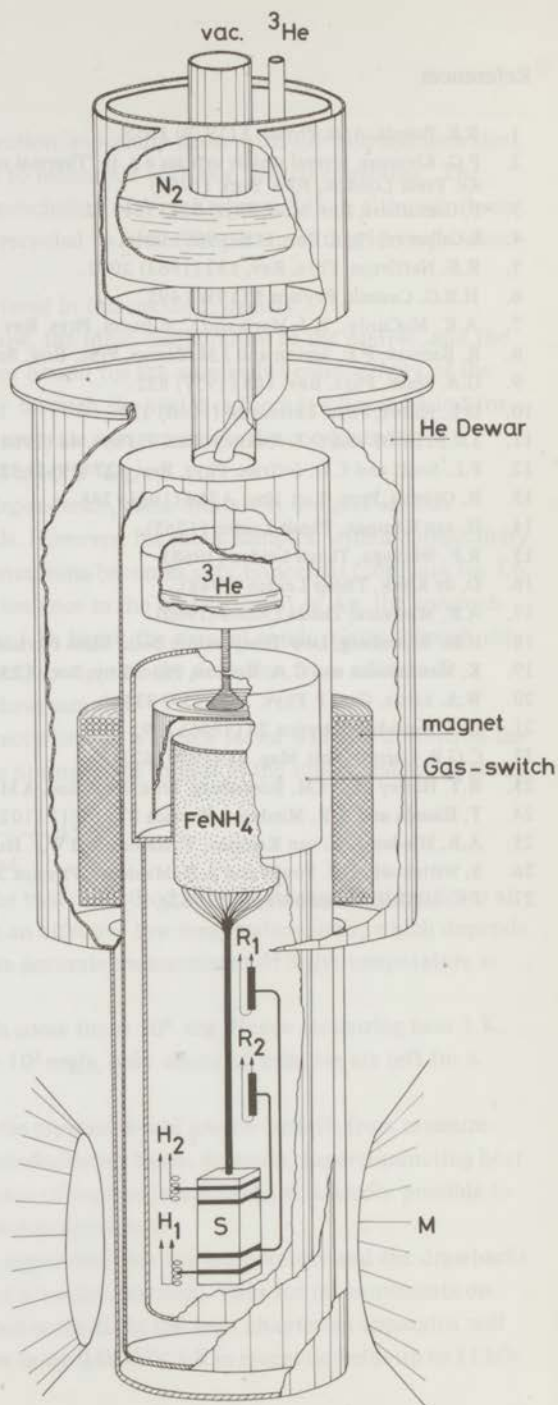
- c. The cooling capacity of a cooling salt is some times 10^5 erg. Hence measuring near 1 K, with consequent heat flows of roughly 10^3 erg/s, only about 10 minutes are left for a conductivity measurement.
- d. The interpretation of results on magnetic crystals would greatly benefit from measurements of the field dependence of the conductivity. Since, however, superconducting heat switches cease to function in the presence of large external fields, it is hardly possible to measure field dependences with our 'switch apparatus'.

The lower limit for the conductivity, the upper limit for the temperature and the drawbacks c and d, are consequences of the choice of a 'switch method'. Thus for measurements on magnetic crystals one would prefer another method. In the next chapter an apparatus will be described, which covers the temperature range $0.05 < T < 5$ K in magnetic fields up to 11 kOe.

References

1. R.E. Peierls, *Ann. Physik* **3** (1929) 1055.
2. P.G. Klemens, several review articles e.g. in 'Thermal conductivity' ed. R.P. Tye, Ac. Press London, New York (1969)
3. P. Carruthers, *Rev. Mod. Phys.* **33** (1961) 92.
4. J. Callaway, *Phys. Rev.* **113** (1959) 1046.
5. R.E. Nettleton, *Phys. Rev.* **132** (1963) 2032.
6. H.B.G. Casimir, *Physica* **5** (1938) 495.
7. A.K. McCurdy, H.J. Maris and C. Elbaum, *Phys. Rev. B* **2** (1970) 4077.
8. R. Berman, F.E. Simon and J.M. Ziman, *Proc. Roy. Soc. A* **220** (1953) 171.
9. G.A. Slack, *Phys. Rev.* **105** (1957) 832.
10. D.L. Huber, *Phys. Letters* **20** (1966) 230.
11. J.C.F. Brock and D.J. Huntley, *Can. J. Phys.* **46** (1968) 223.
12. P.L. Scott and C.D. Jeffries, *Phys. Rev.* **127** (1962) 32.
13. R. Orbach, *Proc. Roy. Soc. A* **264** (1961) 248.
14. H. van Kempen, Thesis Leiden (1965).
15. R.F. Wielinga, Thesis Leiden (1968).
16. D. de Klerk, Thesis Leiden (1948).
17. A.R. Miedema, Thesis Leiden (1960).
18. H.M. Rosenberg, *Low Temperature Solid State Physics*, The Clarendon Press Oxford 1965.
19. K. Mendelsohn and C.A. Renton, *Proc. Roy. Soc. A* **230** (1955) 157.
20. W.A. Little, *Can. J. Phys.* **37** (1959) 334.
21. D.G. Kapadnis, *Physica* **22** (1956) 159.
22. C.G.B. Garrett, *Phil. Mag.* **41** (1950) 621.
23. R.T. Harley and H.M. Rosenberg, *Proc. Roy. Soc. A* **315** (1970) 551.
24. T. Haseda and A.R. Miedema, *Physica* **27** (1961) 1102.
25. A.R. Miedema, H. van Kempen, T. Haseda and W.J. Huiskamp, *Physica* **28** (1962) 119.
26. S. Wittekoek, N.J. Poulis and A.R. Miedema, *Physica* **30** (1964) 1051.
27. J.R. McColl, Thesis Berkeley (1962).

Fig. II.1
 Sketch of the apparatus
 for thermal conductivity measurements
 in the range $0.05 < T < 5$ K.



CHAPTER II

CRYOSTAT COVERING THE RANGE $0.05 < T < 5$ K

II.1 The cryostat and ^3He system

In order to cover the temperature range $0.05 < T < 5$ K both ^3He and demagnetization are used. As a consequence of the sequence of construction, it is possible to use this cryostat either as a ^3He , or as a demagnetization cryostat, or as one in which both systems are used to cover the mentioned range in one run.

The different parts of the apparatus are shown in fig. II.1. The top of the cryostat is cooled with liquid nitrogen; the purpose of this is twofold:

- a. cooling of the electrical leads of the superconducting magnet so as to reduce Joule heating in the leads, and also to minimize the heat leak into the ^4He bath.
- b. cooling of the pumping tubes, which reduces the pumping resistance.

Thermal conductivity measurements could be performed in magnetic fields with the aid of an electromagnet (Bruker BE25C8) giving a field of 11.5 kOe in a pole gap of 8 cm. The magnet, also utilized for N.M.R., produces a stable homogeneous magnetic field, which, for our purpose, is also sufficiently homogeneous over a large volume.

The vacuum can is a 55 cm long, 3.8 cm inner diameter brass tube, and is sealed to its cover by a Wood's metal joint. On the cover, 4 electrovac seals are mounted, so there are 12 feed-throughs for electrical leads into the high vacuum space.

The pumping scheme for the high vacuum and ^3He system is given in fig. II.2. The choice of the diameter of the ^3He pumping-line is rather important. A large diameter is to be preferred when aiming at a low ^3He temperature, but this goes at the expense of a faster ^4He boil off, hence a shorter period of measurement before refill of ^4He . Utilizing the formulae for gas flow¹, the resistance of the pumping-line was estimated. That part of the pumping-line which is inside the cryostat is strongly dependent on the ^4He level. The chosen diameter of the tube in the cryostat (german silver 1.6 cm diameter) is such that with a low ^4He level the resistance in the cryostat is about the same as the resistance between the pump and the top of the cryostat. The tube in the high vacuum is stainless steel (0.6 cm diameter, wall thickness 0.05 cm). Due to the poor thermal conductivity of stainless steel (compare section I.6) the heat leak into the ^3He bath was estimated to be 10-20 erg/s.

The result of the foregoing is that in our ^3He system, in a single shot, a steady temperature of 0.28 K can be reached. This temperature was measured with a magnetic (CMN) thermo-

meter (and heater) connected to the ^3He can.

Also important, apart from the ultimate temperature, is the cooling capacity. To improve the thermal contact with the ^3He , the copper bottom of the can is corrugated. The cooling capacity is shown in fig. II.3, the line is an idealized case (without heat leak), the result of several measurements.

Fig. II.2

Pumping scheme

- ⊗ valves
- ⊗ butterfly valves
- B ionisation manometer (Balzer IMR 3)
- 1. ^3He container (1.5 l gas n.t.p.)
- 2. rotary pump for ^3He system (Balzer Duo I)
- 3. diffusion pump for ^3He system (Edwards EM 2)
- 4. ^3He can in the cryostat
- 5. diffusion pump for high vacuum (Leybold)
- 6. rotary pump for high vacuum (Edwards ES 150)

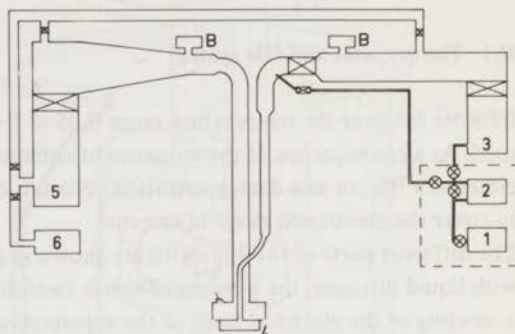
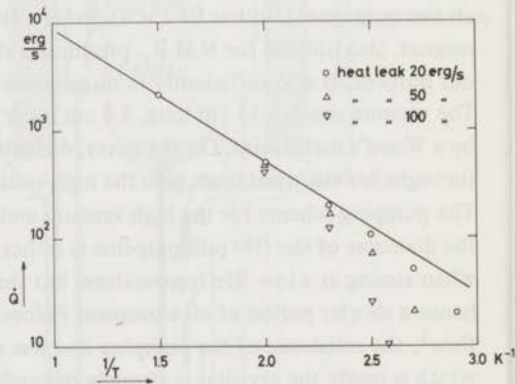


Fig. II.3

Heat flow to the liquid ^3He versus inverse temperature of the ^3He can, representing the cooling capacity of the ^3He system.



II.2 The superconducting magnet

The superconducting magnet is a coil on a stainless steel coilform- (inner diameter 4 cm, outer diameter 6 cm, 10 cm long), which is fixed with two clamps onto the brass vacuum can. The coil consists of 24 layers of 275 turns NbZr wire (supercon, 0.01 inch diameter, copper plated and insulated). The coilform and each layer are mutually isolated with mylar, to prevent a short-circuit within the coil.

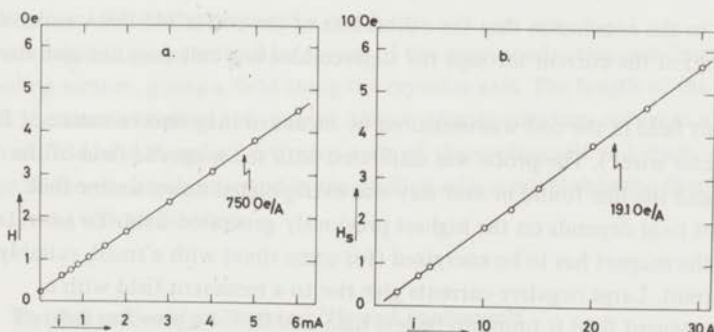
The magnet is energized by a 0-10 V, 0-100 A, $1 : 10^5$ stabilized power supply (Hewlett and Packard). The electrical leads consist of two strands of copper wire (0.03 diameter and 10 each). The coil may be short-circuited at the top of the cryostat, which serves to demagnetize the cooling salt; in this way the field decrease takes place gradually ($\Delta H/H$ is constant), thereby minimizing the eddy current heating in the metal parts. This is particularly important if the cooling salt is already partly demagnetized, i.e. in the low field region. The maximum current is found to be about 35 A, this limit being primarily due to Joule heating in the electrical leads.

The field per unit current in the center of the coil may be calculated from $l=0.1$ m, $\bar{r}=0.025$ m and $N=6.6 \times 10^3/\text{m}$ leading to 740 Oe/A. At room temperature the field was measured with a Hall probe and found to be 750 Oe/A (fig. II.4a).

Fig. II.4

Calibration of the superconducting magnet

- magnetic field H in the center of the coil, measured with the coil at room temperature.
- strayfield H_s from the coil, measured with the coil at liquid He temperature, $H=39.0 H_s$.



In the superconducting state the coil was checked in two ways:

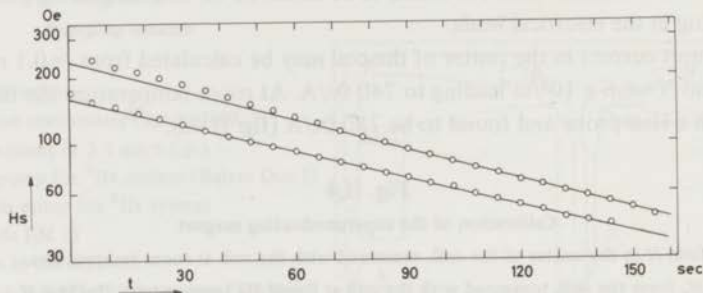
- By measuring the strayfield one may find the field in the center of the coil. In fig. II.4b the strayfield H_s at 6 cm outside the center of the coil is given as a function of the current. The resultant value of the field in the center of the coil (744 Oe/A) agrees quite well with the room temperature value.
- The inductance of the coil may be measured by the rise time of the current or by short-circuiting the coil and measuring the magnetic field (current) decay time. In the latter case one expects

$$\Delta t = \frac{L}{R} \log \frac{I_1}{I_2} = \frac{L}{R} \log \frac{H_{s1}}{H_{s2}}$$

Fig. II.5 shows $\log H_s$ versus t , which is not a straight line; this is probably due to Joule heating of the electrical leads by which R becomes I dependent. From the curves we found $L = 1.1 \pm 0.1H$ corresponding to the calculated value $L = 1.2 H$.

Fig. II.5

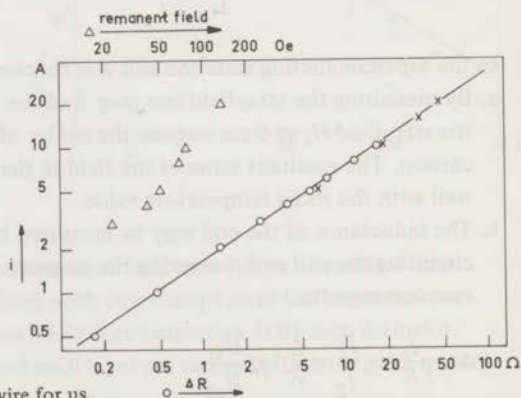
Decay of the (stray) field from the coil as a function of time, after short-circuiting at $t = 0$.



The foregoing leads to the conclusion that the calibration of the coil is 745 Oe/A and even a fast rising (lowering) of the current through the superconducting coil does not give rise to any problems.

Finally, the remanent field in the coil was measured by means of magnetoresistance of Bi (≈ 5 cm, 0.04 diameter wire*). The probe was calibrated with the magnetic field of the coil (see fig. II.6), and the line found in that way was extrapolated down to low field values. The remanent field depends on the highest previously generated field. To get rid of this remanent field the magnet has to be energized (for some time) with a small, suitably chosen, negative current. Large negative currents give rise to a remanent field with a reversed sign. The remanent field is found to be less than 200 Oe for a previous field of 20 kOe (see fig. II.6).

Fig. II.6
Calibration of the bismuth magnetometer
(lower curve), and remanent field
versus highest previously generated current
(upper curve).



* We thank mister C.E. Snel for preparing the Bi wire for us.

II.3 The cooling salt

As a cooling salt usually one of the alums is used. In our case, a large specific heat is more important than the ultimate temperature that can be reached, hence our choice of $\text{FeNH}_4(\text{SO}_4)_2 \cdot 12\text{H}_2\text{O}$ instead of CrK-alum.

The known possibilities for the construction of a cooling salt are:

- a. Single crystals between metal plates parallel to the magnetic field. As a consequence of the boundary resistance the contact area is of crucial importance for the heat transfer to the cooling salt. In our case this area would be about 60 cm^2 .
- b. Powder, mixed with grease and a brush of Cu wires for thermal contact. In this case the contact area is variable, and it is not difficult to make it as large as, for instance, 150 cm^2 . As a consequence of the use of grease, the amount of paramagnetic salt per cm^3 is considerably reduced.

We found that, using FeNH_4 -alum, it is possible to make a cooling salt with the high packing density of case a and the large contact area of case b. When FeNH_4 -alum is heated up to about 50°C the crystal melts (that is, it forms a solution with its own crystal water). By inserting a brush of copper wires before recrystallization, it is possible to reach a satisfactory combination of the advantages of a and b.

The cooling salt is magnetized by means of the superconducting coil described in the preceding section, giving a field along the cryostat axis. The length of the cooling salt is about the same as that of the magnet. Hence demagnetization occurs in a rather inhomogeneous field, and therefore different parts of the cooling salt will reach different temperatures. Since the brush, inserted in the cooling salt, reestablishes the thermal equilibrium, this is not a serious problem.

II.4 The thermal contact between ^3He and cooling salt

There should be a thermal connection between the ^3He bath and the cooling salt, in such a way that its conduction is poor when the salt is demagnetized ($T < 0.3 \text{ K}$) and good otherwise. In that way the ^3He is used most effectively and for the high temperature measurements, it is possible to cool the sample with the aid of the large heat capacity of the liquid ^3He .

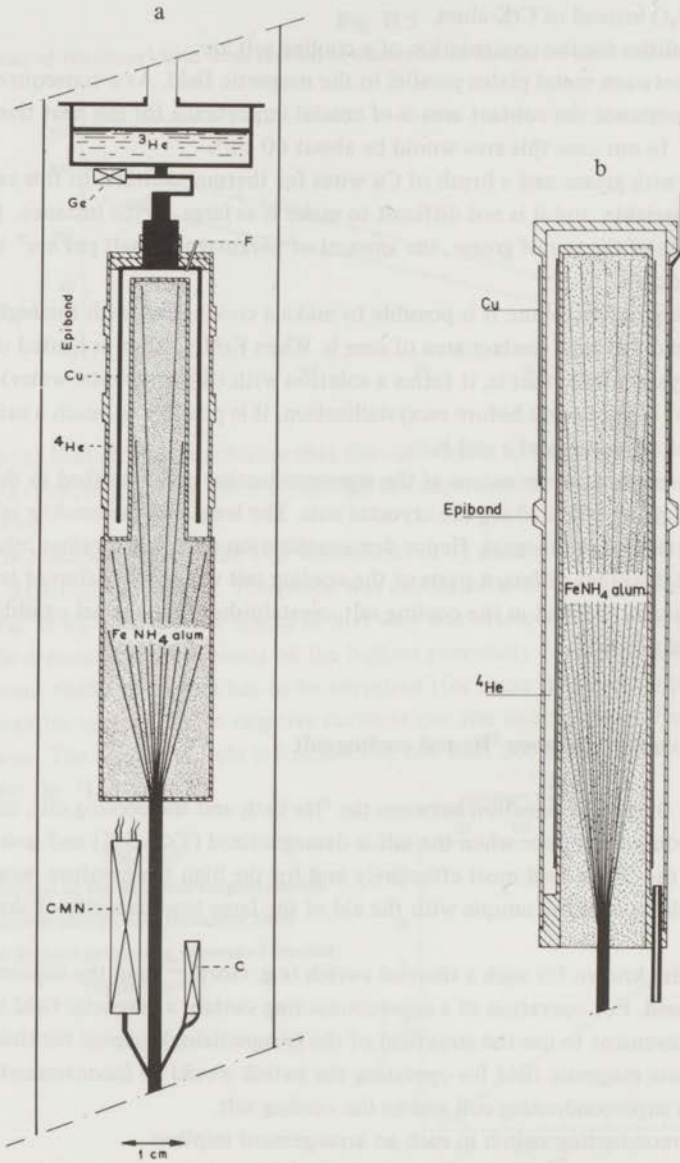
Several solutions are known for such a thermal switch (e.g. Gorter²) and the superconducting switch is widely used. For operation of a superconducting switch, a magnetic field is necessary. It is convenient to use the strayfield of the (magnetizing) magnet for this purpose. Moreover, a separate magnetic field for operating the switch would be inconveniently close to the field of the superconducting coil and to the cooling salt.

The use of a superconducting switch in such an arrangement implies:

- a. The switch stays in the superconducting, i.e. thermally isolating, state, more or less

Fig. II.7

Construction of a gas-switch, the cooling copper shield being inside (a) or outside (b) the gas space



independently of temperature. Hence one would not be able to benefit from the cooling capacity of the ^3He for the measurements above 0.4 K.

- b. Isolation of the cooling salt from the ^3He occurs merely at low field values, hence fast demagnetization is necessary.
- c. If either the remanent field is too large, or normal enclosures in the bulk of the superconductor occur, the switch will not break thermal contact.
- d. The choice of the geometry of the switch is necessarily a compromise, since a short, thick connection is desirable to carry off the heat of magnetization; while on the other hand a long, thin connection is desired to reduce the heat leak after demagnetization.

Point a is a particularly serious drawback for thermal conductivity measurements. In fact, we found it to be very difficult to measure thermal conductivity between 0.5 K and 0.9 K using a superconducting switch.

An alternative solution is provided by the thermal conductivity of ^4He gas. From the saturated vapour pressure versus temperature relation of ^4He , one may expect a reasonable heat transport by ^4He gas down to about 0.35 K. At demagnetization temperatures ($T < 0.1$ K) the saturated pressure is quite low, hence there is negligible heat transport by ^4He gas. Provided the amount of ^4He is small, the condensed gas (presumably as a superfluid film on the walls of the holder) will not give rise to an appreciable heat transport either. For the construction of a 'gas-switch', epibond 100 A³ is a very suitable material, in view of its poor thermal conductivity⁴. Epibond 100 A is commercially available as a powder, which melts to a thick fluid upon heating, and which hardens (for example in 24 hours at 122°C) to a machinable ingot. Precautions need to be taken in order to prevent formation of small bubbles in the bulk of the epibond. We found as a convenient solution for this problem:

- a. Melt the powder at 100°C and pump on the fluid until it is free of gas (mostly air).
- b. Pour the degassed epibond in teflon matrices for hardening. Teflon was chosen since it is one of the very few materials that does not adhere to the epibond.

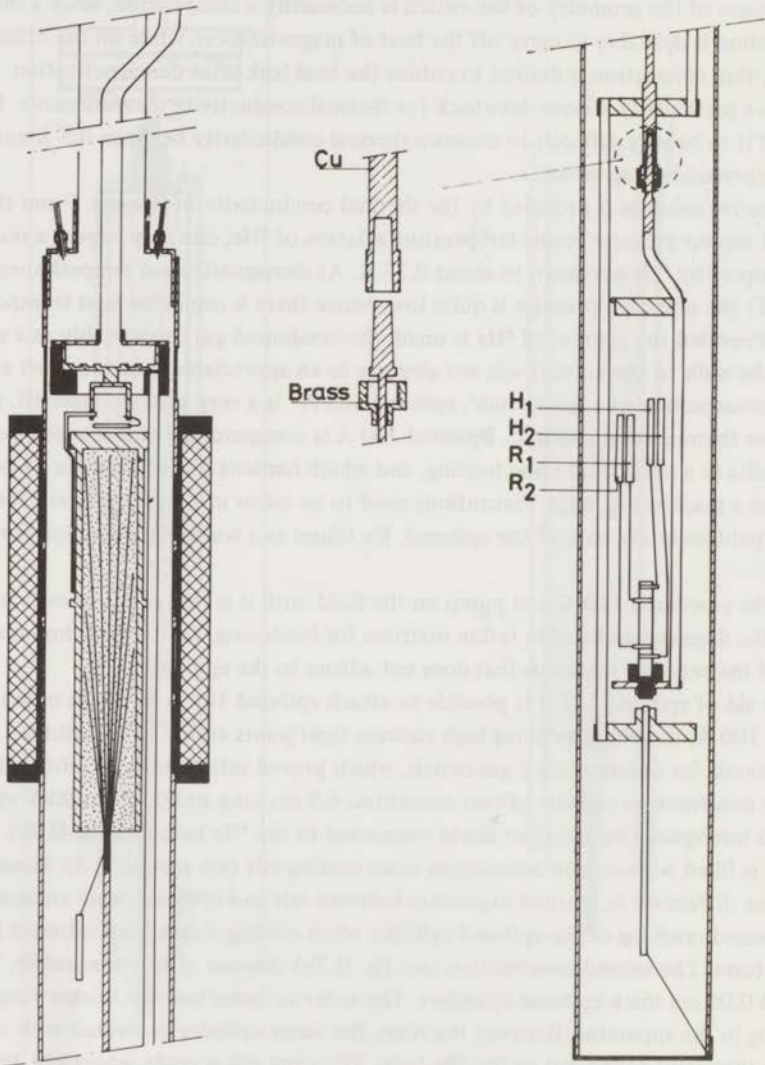
With the aid of epibond 121 it is possible to attach epibond 100 A to pieces of metal or to epibond 100 A, thereby producing high vacuum tight joints at low temperatures.

Two methods for constructing a gas switch, which proved satisfactory, are shown in fig. II.7. The first construction consists of two concentric 4.5 cm long and 0.05 cm thick epibond cylinders interspaced by a copper shield connected to the ^3He bath (see fig. II.7a). The inner cylinder is filled with an iron ammonium alum cooling salt (see section II.3). Some problems, due to the difference in thermal expansion between salt and epibond, were encountered, which caused cracking of the epibond cylinder when cooling down from nitrogen to helium temperatures. The second construction (see fig. II.7b) consists of two concentric, 12 cm long and 0.05 cm thick epibond cylinders. The outer cylinder has two thicker rings, for mounting in the apparatus. Between the rings, the outer cylinder is covered with copper foil, which is thermally connected to the ^3He bath. The alum pill is made separately, leaving some space for shrinkage of the epibond. With the aid of Apiezon N grease the pill is stuck

Fig. II.8

Inner apparatus of the equipment for measuring thermal conductivity between 0.05 and 5 K.

The screwed thermal connection is shown on an enlarged scale.



in the epibond cylinder. In both cases, the gas space has thoroughly been tested at room and nitrogen temperature, and afterwards filled with 0.1 atm ^4He gas.

The performance of the second construction is less effective than that of the first one. The cooling of the magnetized cooling salt for the second case takes about five times the cooling time for the first one (about 5 minutes). A discussion of the performance of gas switches will be given in section IV.2.

II.5 Apparatus mounting and sample holder

As shown in fig. II.8, the inner apparatus is mounted in a frame consisting of three german silver capillaries. The upper ends of the capillaries are soldered to a brass ring, which is fastened to the ^3He can. The frame is strengthened by a number of epibond rings. The lower end of the capillaries are fastened to an epibond disk. A stainless steel tripod is screwed into the middle of this disk in order to center the frame in the vacuum can. A cylindrical thermal shield, consisting of coil-foil (in this case copper wire on mylar), surrounds the frame. This shield is thermally grounded to the ^3He bath.

The tripod causes a continuous heat leak from the vacuum can, at about 1 K, to the ^3He bath. To get an idea of the temperature of the thermal shield, we measured the temperature of the disk by a carbon resistor, which was found to be below 0.45 K during the whole experiment; the same will certainly be true for the thermal shield.

Several sample holders have been used. The last version is shown in the figure. Thermal connections to crystalline samples were made by glueing copper foil to the sample with 'Bisonkit'⁵. The use of 'Bisonkit' appeared to give better results than mounting with 'Apiezon N', probably because it is difficult to fasten the small copper foils reliably to the crystal surfaces. The samples were glued in a brass foot, which is screwed onto the copper bottom of the sample holder.

The copper bottom is cooled by a copper rod, connected to the central rod, which in turn is cooled by the brush of the cooling salt. The sample holder is surrounded by a coil-foil cylindrical thermal shield, which is also connected to the central rod. Hence the wall of the sample holder is colder than, or at least equal to, the temperature of the sample itself.

The top of the sample holder is an epibond disk having a number of feedthroughs; the thermometers and heaters are mounted in the sample holder. The electrical connections to the feedthroughs are made of 0.005 cm diameter 'constantan' wire. The mounting of thermometers and heaters can be left intact while interchanging samples. This is important for a proper analysis of the data, since in this way, heat leak and parallel conductivity along the electrical leads remain unaltered.

It is undesirable to solder the sample holder rod to the central rod, since the heat needed to make a reliable joint, may ruin the sample and/or the cooling salt. Moreover, the use of (soft) solder should be avoided, since it becomes superconducting, which causes additional

thermal resistance. We therefore tried a method by which the sample holder rod is screwed to the central rod. Our design for such a thermal connection (see fig. II.8) consisted of a copper cone in a conical 'house', fixed with a brass nut. This construction has several advantages:

- a. Large contact area in spite of small dimensions.
- b. Due to the larger thermal expansion of brass compared to copper, cooling will press the cone tightly into the house.
- c. It is a rigid, mechanically strong connection.

Some Apiezon N grease was put onto the surface of the cone before mounting to facilitate disconnection and to prevent oxidation of the copper.

The thermal conductivity of the cooling rod, including the thermal connection, was determined in a separate experiment and found to agree with the value calculated for a copper rod without interruption.

References

1. R. Jaeckel, *Handbuch der Physik*, part 12 (1956) 606.
2. F.W. Gorter, Thesis Amsterdam (1969).
3. 'Epibond', Furane Plastics Inc.
4. A.C. Anderson, W. Reese and J.C. Wheatley, *Rev. Sci. Instr.* **34** (1968) 1386.
5. 'Bisonkit', contactadhesive. Perfecta Chemie N.V., Goes, Holland.

CHAPTER III

TEMPERATURE MEASUREMENT AND CONTROL

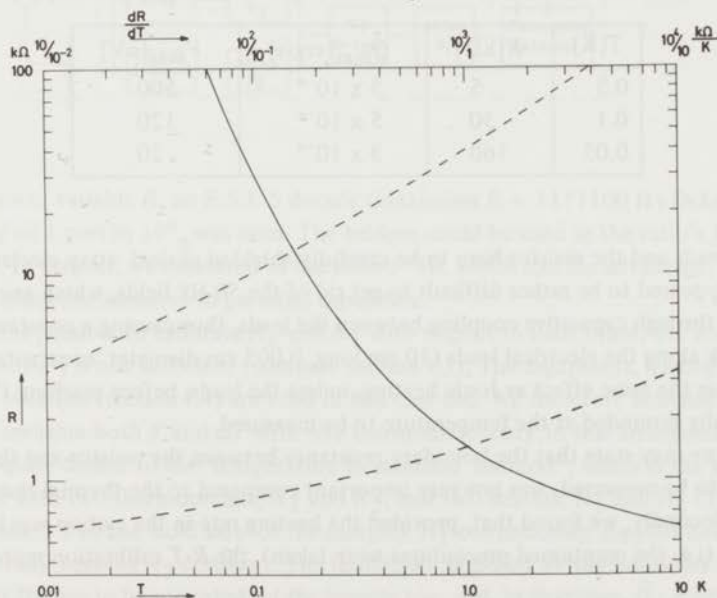
III.1 Carbon resistance thermometry

The purpose of the experimental arrangement, described in the previous chapter, is to measure thermal conductivity of crystals in magnetic fields; the use of magnetic thermometry is therefore hardly possible. Several authors¹⁻⁴ showed Speer carbon resistors to be useful down to very low temperatures. Their conclusions were:

- a. neither R nor $\frac{dR}{dT}$ becomes prohibitively large even at low temperatures (see fig. III.1).
- b. the resistance is only slightly sensitive to magnetic fields.
- c. the R - T calibrations reproduce quite well, if electrical and thermal connections to the resistors are handled with care.

Fig. III.1

Calibration of a Speer resistor. The full curve represents the resistance versus temperature, the dashed curve the resistance versus the temperature derivative of the resistance.



A disadvantage of resistance thermometry is the Joule heating in the resistor. For a given amount of heat, developed per unit time, \dot{Q} , the mean temperature T_c of the carbon is a function of the surface temperature T (i.e. the temperature to be measured), and the thermal resistance causing a difference between T_c and T . This thermal resistance is due to:

- a. The boundary resistance between the surface of the carbon and the cooling surface (e.g. coil-foil). The contact area will be about 0.5 cm^2 and consequently

$$\dot{Q} = 5 \times 10^4 (T_c^4 - T^4) \text{ erg/s.}$$

We require for our thermometer $T_c - T < 10^{-3} T$; hence $\dot{Q} < 200 T^4 \text{ erg/s.}$

- b. The thermal resistance in the carbon of the thermometer. Assume

$$\dot{Q} = cT^3 (T_c - T).$$

Substitution of the mentioned requirement leads to $\dot{Q} < c 10^{-3} T^4$.

The constant c may be found from experimental data. This was done by measuring the power dependence at 0.1 K by varying the voltage of the Wheatstone bridge, resulting in $c = 50 \text{ erg/s K}^4$. Joule heating in the resistor due to the bridge voltage has therefore to be smaller than $0.05 T^4 \text{ erg/s.}$

This very low admissible power level has the following consequences:

- a. The power level of the Wheatstone bridge has to be kept quite low, as is shown in the table:

$T[\text{K}]$	$R[\text{k}\Omega]$	$\dot{Q}_{\text{max}}[\text{erg/s}]$	$V_{\text{max}}[\mu\text{V}]$
0.3	5	5×10^{-4}	500
0.1	30	5×10^{-6}	120
0.05	160	3×10^{-8}	20

- b. Both the leads and the resistor have to be carefully shielded against stray electromagnetic fields. It appeared to be rather difficult to get rid of the 50 Hz fields, which are probably picked up through capacitive coupling between the leads, thus causing a constant current.
- c. A heat leak along the electrical leads (10 cm long, 0.005 cm diameter 'constantan') would cause the same effect as Joule heating, unless the leads, before reaching the carbon, are thermally grounded at the temperature to be measured.

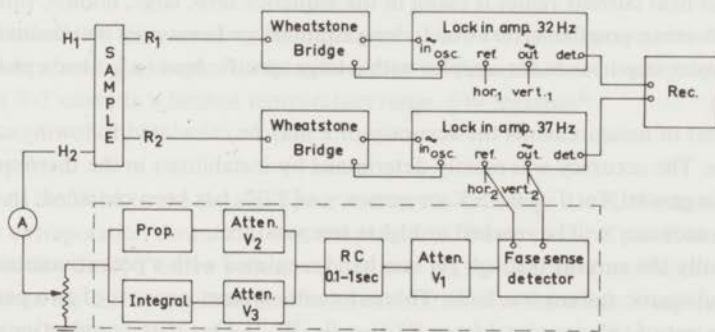
Concluding, we may state that the boundary resistance between the resistor and the temperature to be measured, was not very important compared to the thermal resistance in the carbon. Secondly, we found that, provided the heating rate in the carbon was less than $0.05 T^4 \text{ erg/s}$ (i.e. the mentioned precautions were taken), the R - T calibration reproduced quite well.

III.2 Procedure of the measurement

For a measurement of the thermal conductivity, i.e. the average conductivity in a certain interval of temperature, either two temperatures or one temperature and a temperature difference have to be determined. This was done with the aid of two Speer carbon resistors. The resistances of the carbon resistors were measured by means of two Wheatstone bridges, operating at low frequency (28 and 31 Hz). Alternating currents have the advantage that the generation of thermal voltages are avoided, but on the other hand low frequencies are required to limit losses in the metal parts of the apparatus. Moreover, with low frequency alternating current, it is easier to meet the requirements of the preceding section. Detection is made with lock-in amplifiers (see fig. III.2).

Fig. III.2

Block-diagram of the measuring system and heater circuit.



For the known, variable R , an E.S.I. 5 decade (maximum $R = 1111100 \Omega$) Dekabox, with an accuracy of 1 part in 10^4 , was used. The bridges could be used in the ratios 1:1, 1:10, and 1:100. In general, we measured in the ratio 1:10, which has the advantage, compared to 1:1, of being less sensitive to parasitic capacities.

Although it is possible to calibrate R_1 and R_2 with respect to each other, the accuracy obtained ($3 \cdot 10^4$) is not sufficient (compare section I.3). The arguments, leading to the use of thermal switches (section I.4) are valid in this case too. We therefore searched for a method to measure both T and ΔT with one thermometer only, in this arrangement. The solution is quite similar to the 'temperature to standard' method⁵, wherein the conductivity is measured with two thermometers, R_1 and R_2 , and two heaters, H_1 and H_2 (1 refers to the 'warm side', 2 to the 'cold side' of the sample). H_2 continuously supplies heat to the sample, thereby keeping R_2 constant. The limitation, imposed by the boundary resistance, implies that H_2 has to be mounted on the sample too, and, in that case, \dot{Q}_2 is of the same

order of magnitude as the maximum heat flow through the sample (compare with section I.3). Hence, in the low temperature region, the cooling salt will not warm up much faster than in a thermal conductivity measurement using one heater only.

Varying \dot{Q}_1 and keeping R_2 constant by appropriate adjustment of \dot{Q}_2 , the temperature differences may be obtained from R_1 only. A chosen set of heat current values through the sample give rise to a corresponding set of temperature differences, which can be plotted in a graph. The slope of the resulting line is the thermal conduction of the sample. The magnitude of \dot{Q}_1 is limited by \dot{Q}_2 (with $\dot{Q}_1 = 0$). The magnitude of \dot{Q}_2 is related to the sample temperature chosen, and to the thermal resistance between sample and cooling reservoir. This method, in which λ is derived from a set (in general 3) of heat current values, has several advantages:

- Since the slope of the \dot{Q}_1 versus ΔT graph is insensitive to heat leaks, it is possible to measure with very small heat currents through the sample (heat currents smaller than 10^{-2} erg/s can be actually used).
- If the set of heat current values is taken in the sequence zero, large, middle, small and zero heat current, possible errors due to long equilibrium times may be eliminated. This is of particular importance for samples with a large specific heat (e.g. near a phase transition).
- From the set of measurements the accuracy of λ may be calculated following standard procedures. The accuracy was mainly determined by instabilities in the thermometer readings. In general, for $T > 0.15$ K an accuracy of 2-3% has been obtained. In magnetic fields, this accuracy will be reached at higher temperatures.

Whereas initially the current through H_2 was hand-regulated with a potentiometric circuit, later on an automatic system was built. This automatic system consists of two parts, both driven by the out-of-balance signal from R_2 (see fig. III.2). One part, 'proportional regulation', compensates fast thermal variations (e.g. vibrations due to a shock). The other part, 'integral regulation', compensates drift in the temperature (e.g. due to warming up of the cooling salt).

Both the specific heat and the thermal conductivity may vary strongly over the whole temperature range of the experiments, and also the sample characteristics may be quite different. For measurements under such different circumstances, the time constants of the heater circuit must be correspondingly adjusted. This can be realized by the variable attenuators V_1, V_2, V_3 , and a variable RC -time.

The electronic design is such that the heater circuit does not change the heater current for an out-of-balance of less than 1 mV and an attenuation factor 100. Usually $\frac{\Delta R}{R} = 3\%$ corresponds to an out-of-balance of about 300 mV. Hence the heater circuit compensates up to $\frac{\Delta R}{R} = 10^{-4}$. Under favourable circumstances (i.e. large specific heat and/or large conductivity) this may be improved up to 10^{-6} .

During the experiment, the out-of-balance signals of the lock-in amplifiers were continuously recorded. Instead of \dot{Q}_1 versus ΔT , \dot{Q}_1 versus the out-of-balance signal Δu of the lock-in

measuring R_1 was used for computation of λ . This simplified the computation, but introduced a systematic error due to the non-linearity of the Wheatstone bridge. If $\Delta R/R \approx 5\%$, this error was found to be about 1%, and depended slightly on the value of R .

Another systematic error was due to the use of a single value of $\frac{dR}{dT}$ for the set of values for one point. The magnitude of this error depends strongly on $\frac{\Delta R}{R}$ and $\frac{d^2R}{dT^2}$, but did not exceed 1% in the actual measurements.

The systematic errors, introduced by using Δu instead of ΔT were within the accuracy of the measurement. It is possible to improve the accuracy (especially above 0.25 K), but in that case the systematic errors would have to be avoided. An interesting possibility is an automatic circuit for H_1 , driven by R_1 . In that case, one would measure with a balanced circuit for R_1 , and it is possible to choose ΔT (that is ΔR) instead of \dot{Q}_1 .

III.3 R - T calibration and magnetic thermometry

Carbon thermometers are secondary thermometers, and as far as is known, the R - T curve cannot be described by a simple formula. A number of formulae have been proposed, to describe the R - T curve in a limited temperature range. For instance⁶

$$\log \frac{R}{R_0} = \frac{A}{\sqrt{T}},$$

can quite well be fitted to the data of Speer resistors in the range 1-4 K. We have tested this formula for extrapolation down to lower temperatures. Down to 0.1 K the formula was found to describe the R - T curve with an accuracy of 5%, which was insufficient for our purpose. Hence the carbon resistors had to be calibrated over the whole temperature range. The results can be expressed in tabular form, but for interpolation, and in particular also for the purpose of computer handling of the data, an analytic expression is advantageous. Therefore the formula⁷

$$\log R = \sum_{i=1}^n a_i \log^{i-1} T, \text{ where } n \text{ is } 10 \text{ or } 12,$$

was fitted to the experimental data in the range $0.05 < T < 5$ K. The a_i values found in this way were used for the computation of the thermal conductivity. At regular time intervals the R - T calibration was rechecked, and the a_i were found to reproduce within several percents.

As mentioned in section III.1, the requirements for carbon resistance thermometry are rather high. Consequently it is desirable to calibrate the resistors in exactly the same situation as in the actual measurements. We therefore constructed a Ce-Mg nitrate susceptibility thermometer of such a size that it could replace the sample. For the susceptibility measurements, a commercial⁸ low frequency (21 Hz) mutual inductance bridge was used.

The familiar construction of a set of inductance coils outside the vacuum space is subject to

serious objections if only small susceptibilities are to be measured. A construction in which the coils are mounted onto the CMN has several advantages:

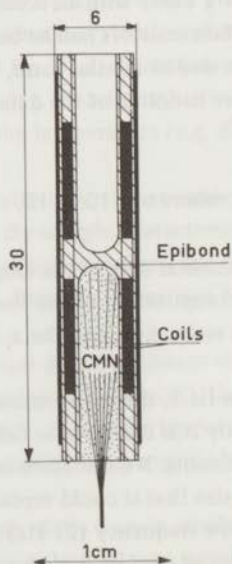
- optimum filling factor.
- parasitic susceptibilities of the construction materials are kept to a minimum.
- as a consequence of the small diameter of the coils, the influence of other magnetic materials (e.g. cooling salt) will be unimportant.
- condensation of air (oxygen) on the coils will be avoided by mounting the thermometer in the high vacuum (parasitic oxygen can be one of the most important origins of errors in the calibration).

A disadvantage of such a thermometer is that a current through the coils causes Joule heating. This was avoided by using superconducting wire (Nb) for the primary coil, and by measuring with a balanced bridge, in which case the current through the secondary coil is zero.

In fig. III.3 such a magnetic thermometer is shown. The secondary consists of two, oppositely wound coils (14 layers of 125 turns each, 0.005 cm diameter Cu wire). The primary consists of one layer of 450 turns of 0.005 cm Nb wire, having at both ends 30 additional turns to improve the homogeneity of the primary field. One half of the inner part of the thermometer (with a total length of 3 cm and 0.6 cm diameter) is filled with 0.14 g 'molten' CMN (compare the construction of the cooling salt section II.3). The total weight of the thermometer is 2 g and the total specific heat is estimated to be

$$c_{\text{therm.}} = 0.15 T^{-2} + 3 T + 80 T^3 \text{ erg/K.}$$

Fig. III.3
Magnetic thermometer, used as calibration standard
between 0.05 and 5 K.



The calibration to the ^4He temperature scale is found to be reproducible, within 1%. For CMN the Curie-Weiss θ will be mainly determined by the form factor of the sample; in our case θ is estimated to be less than 1 mK. Hence, in the temperature range of our experiments, Curie's law will provide a sufficiently accurate (at the lowest temperatures the error is about 1%) relation between the susceptibility readings and the absolute temperature of our thermometer.

This magnetic thermometer serves as a calibration standard, and all temperatures mentioned in the following chapter, although measured with Speer resistors, refer to this Curie law thermometer.

III.4 Magnetic field dependence of Speer resistors

Some results on the magnetic field dependence of Speer resistors are reported in the literature^{2,3}. However, for our purposes $R(H)$ should be known to a higher accuracy. We therefore measured the field dependence of a Speer resistor (R_1 see fig. III.2) in a separate experiment, similar to that described by Mess³.

The resistor (R_1) was mounted close to the CMN susceptibility thermometer. A second resistor (R_2) was mounted 26 cm from R_1 . Hence with R_1 in the center of the magnet, R_2 was merely influenced by the stray field, which is about 6% of the field strength in the center of the magnet. Several runs in different magnetic fields were taken, according to the procedure:

a. R_1 and R_2 were calibrated to each other and (in zero field) to the CMN thermometer.

In fig. III.4 this R - T calibration is compared to the calibration measured in the other apparatus (section III.3). Starting from a certain susceptibility χ_1 , this corresponds to a certain resistance of the carbon resistor, which in turn is related to a particular value of χ_2 . For a χ_1 versus χ_2 graph, one expects a straight line, the slope being the ratio of the two slopes in the χ_1, χ_2 versus $1/T$ graphs. The agreement was found to be about 1‰.

The largest susceptibilities in fig. III.4 correspond to a temperature of about 0.08 K.

b. In a magnetic field $R_1(H)$ was calibrated against R_2 .

c. The, strayfield corrected, R_2 value was used to derive $R_1(0)$.

The resultant field dependence is shown in the table.

H [kOe]	T range [K]	R range [k Ω]	$\frac{\Delta R}{R}$
0.9	0.05 - 2	1 - 120	$9 \times 10^{-4} R^{1.0}$
3.9	0.08 - 2	1 - 45	$3.9 \times 10^{-3} R^{0.92}$
8.0	0.12 - 2	1 - 25	$8.0 \times 10^{-3} R^{0.79}$
12.0	0.10 - 2	1 - 30	$1.3 \times 10^{-2} R^{0.76}$

In the last column R is given in k Ω .

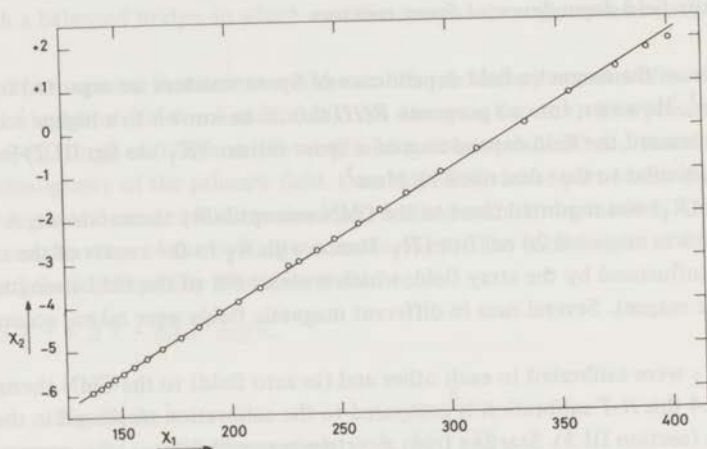
For the mentioned temperature and resistance range the combined data may be expressed as

$$\frac{\Delta R}{R} = -0.10 HR^{1-0.02H} \%$$

where H is the field strength in kOe and R in $k\Omega$. This formula has been used for the correction in the λ measurements.

Fig. III.4

Comparison of two R - T calibrations; the susceptibilities of the two magnetic thermometers are related through the resistance of the Speer resistor.



References

1. J. Nicol and T. Soller, *Bull. Am. Phys. Soc.* 2 (1957) 63.
2. W.C. Black, W.R. Roach and J.C. Wheatley, *Rev. Sci. Instr.* 35 (1964) 587.
3. A.S. Edelstein and K.W. Mess, *Physica* 31 (1965) 1707.
4. O.G. Symko, *Phys. Lett.* 25A (1967) 385.
5. A.R. de Vroomen, *Suppl. Bull. Inst. du Froid, Annexe 1958-1* (1958) 137.
6. J. Rafalowicz and B. Sujak, *Act. Phys. Pol.* 25 (1964) 599.
7. E. Lagendijk, to be published.
8. Cryotronics Inc. mutual inductance bridge, compare W.L. Pillinger, P.S. Jastram and J.G. Daunt, *Rev. Sci. Instr.* 29 (1958) 159.

CHAPTER IV

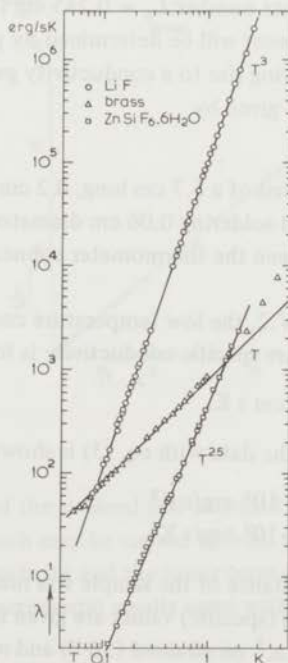
SOME CONSIDERATIONS CONCERNING THE EXPERIMENTAL RESULTS

IV-1 Calibration and test of the procedure

Three samples were chosen to calibrate and test the apparatus, namely a brass rod, a single crystal of LiF, and a single crystal of $\text{ZnSiF}_6 \cdot 6\text{H}_2\text{O}$ (see fig. IV.1). In the low temperature region, the thermal conductivity of brass is expected to be proportional to T ; the absolute value may be found from the electrical resistance, using the Wiedemann-Franz relation. LiF is a diamagnetic crystal, and the dimensions of our crystal were such that a high conduction may be expected. $\text{ZnSiF}_6 \cdot 6\text{H}_2\text{O}$ is also a diamagnetic crystal. The dimensions were chosen in such a way that the conduction of the sample will be quite low. In this case, λ at $T \approx 0.1$ K was measured using heat currents as low as 0.003 erg/s.

Fig. IV-1

The overall conductivities of the three samples used to calibrate and check the apparatus.



With these three samples we obtained a test on the temperature dependence and absolute value for large and small conductivities. The corrections necessary when measuring in magnetic field, may be checked with these samples also, the conductivities being expected to be independent of magnetic field. All this was confirmed, if the field corrections on the thermometry were used.

Brass

The conductivity of metals consists in general of an electronic and a lattice component

$$\lambda = \lambda_e + \lambda_g \quad (1)$$

In the case of alloys, such as brass, the electronic component is rather small, due to a large impurity scattering, and the rôle of electron-phonon interaction would not reflect in λ_e at low temperature. In that case, λ_e is related to the electrical resistance R , as (Wiedemann-Franz)

$$\lambda_e R = L_o T, \quad (2)$$

in which the Lorentz number $L_o = 0.245 \text{ erg } \Omega/\text{s K}^2$.

The lattice component will be determined by phonon-electron interaction and dislocation scattering, both giving rise to a conductivity proportional to T^2 . So we expect the conductivity of brass to be given by

$$\lambda = aT + bT^2. \quad (3)$$

The sample consisted of a 5.7 cm long, 0.2 cm diameter brass wire. The thermal contacts were made by hard soldering 0.06 cm diameter Cu wire in small holes drilled in the brass. The distance between the thermometer connections was 2.48 cm, hence the geometry factor is 79 cm^{-1} .

As shown in fig. IV.2, the low temperature conductivity tends to a linear T dependence; and the low temperature specific conductivity is found to be

$$\lambda = 6.2 \times 10^4 \text{ erg/cm s K}.$$

A comparison of the data with eq. (3) is shown in fig. IV.3. The straight line corresponds to

$$a = (7.85 \pm 0.05) 10^2 \text{ erg/s K}^2$$

$$b = (0.9 \pm 0.2) 10^2 \text{ erg/s K}^3.$$

The electrical resistance of the sample was measured and found to be constant in the range 1-4 K. The various (specific) values are given in the table, and may be compared with the results of Kemp e.a.¹ on strained (30 S) and annealed (30) brass.

	$\mu\Omega$ cm			erg/cm s K	
	ρ_{273}	ρ_{90}	ρ_0	λ_e	λ_g
this experiment	6.49	4.41	3.93	6.20×10^4	7×10^3
30 S	6.9	5.0	4.3	5.7	7.1
30	6.3	4.2	3.6	6.8	5.

Fig. IV.2

Thermal conductivity of brass
as a function of temperature

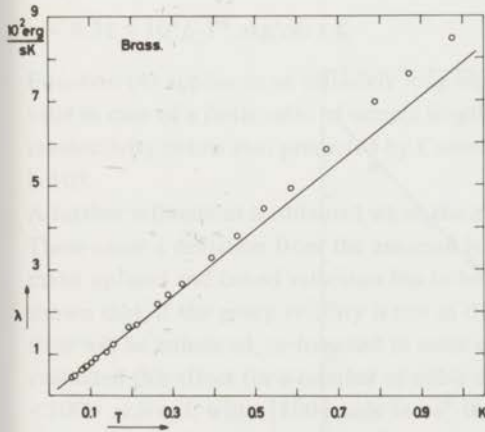
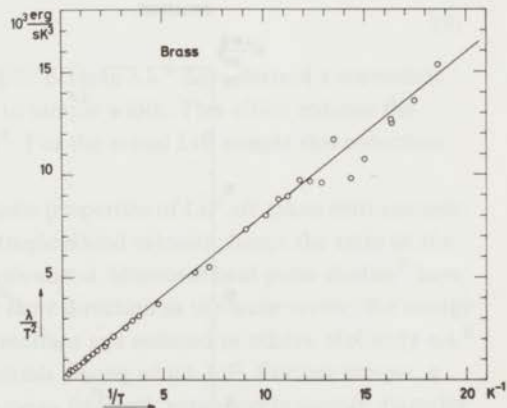


Fig. IV.3

Thermal conductivity of brass,
plotted as λ/T^2 versus $1/T$, so that the
value at $1/T=0$ gives the coefficient
for the lattice part of the conductivity,
and the tangent gives the coefficient of
the electronic part of the conductivity.



Consequently our data lie between the values of the strained and annealed samples of ¹. Our sample appears to be 'partly annealed', which may be caused by hard soldering of the thermal connections. The residual electrical resistivity and the linear term of the thermal conductivity are related by eq. (2), and the experimental results agree with eq. (2) within the accuracy of the measurement.

LiF (sample dimensions: 0.55 x 0.52 x 4.1 cm)

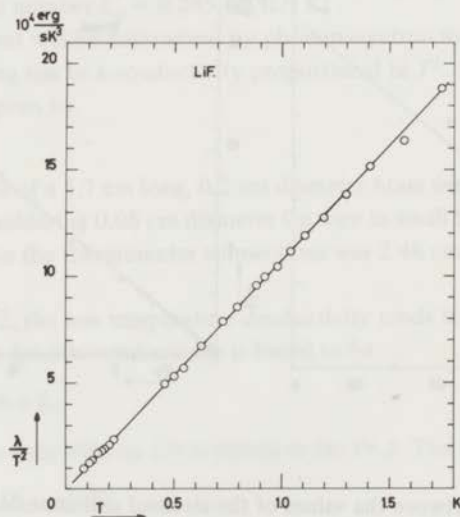
LiF single crystals are often used to study lattice thermal conductivity, because it is a simple (two ions in the unit cell), cubic crystal. Having a high Debye temperature ($\theta_D = 722 \text{ K}^{2,3}$), one may find for LiF a T^3 dependence over quite a wide and easily attainable temperature range. The single crystal was grown at the Harshaw Chemical Company and kindly given to us by prof. Pohl (Cornell University). The thermal connections were (four) small Cu strips, glued around the sample and the crystal was mounted in a brass holder (compare with section II.5).

As is shown in fig. IV.4, a T^3 dependence fits nicely to the data over more than a decade in temperature, and consequently the boundary resistance completely determines the behaviour of λ . The experimental data lead to

$$\lambda = 7.12 \times 10^5 T^3 \text{ erg/cm s K.}$$

Fig. IV 4

Thermal conductivity of LiF, plotted as λ/T^2 versus T , demonstrating that λ is proportional to T^3 in the range $0.08 < T < 1.4 \text{ K}$, with $7.12 \times 10^5 \text{ erg/cm s K}^4$ as proportionality constant.



The specific heat, velocity of sound and elastic constants of LiF are known^{2,3}, hence it is interesting to compare the measured conductivity with the theory of lattice thermal conductivity in the boundary scattering region (section I.1).

The thermal conductivity resulting from Casimir's theory⁴ may be expressed in the form

$$\lambda = \frac{1}{3} c [(\bar{v}^{-2})/(\bar{v}^{-3})] l_C \quad (4)$$

in which diffuse boundary scattering and an infinitely long sample are assumed. As stated in section I.1, the thermal conductivity will be proportional to T^n with $n < 3$ if specular reflection occurs. For our LiF crystal the conductivity appeared to be quite accurately proportional to T^3 , hence we may conclude that reflection was of no importance.

To evaluate eq. (4), one may use the Debye theory, for a monatomic lattice leading to (eq. I.10)

$$\lambda = \frac{1}{3} [1,941 \times 10^{10} \frac{\rho}{M} (\frac{T}{\theta_D})^3] [3,95 \times 10^2 \sqrt[3]{\frac{M}{\rho}} \theta_D] l_C \quad (5)$$

For an s atomic lattice, using the definition of the Debye temperature according to Keesom⁵, the formulae for c , v and λ have to be changed into

$$c_{\text{mol}} = s 1,941 \times 10^{10} (\frac{T}{\theta_D})^3 \text{ erg/K mol}, \quad (6)$$

$$v = 3,95 \times 10^2 \sqrt[3]{\frac{M}{s\rho}} \theta_D \text{ cm/s} \quad (7)$$

$$\lambda = \frac{1}{3} \frac{\rho}{sM} c_{\text{mol}} v l_C \text{ erg/cm s K} \quad (8)$$

Hence for the diatomic lattice LiF, one finds

$$\lambda = 8.32 \times 10^5 l_C T^3 \text{ erg/cm s K} \quad (9)$$

Equation (4) applies to an infinitely long sample; Berman e.a.⁶ have derived a correction valid in case of a finite ratio of sample length to sample width. This effect reduces the conductivity below that predicted by Casimir⁴. For the actual LiF sample this reduction is 10%.

A further refinement is obtained when the elastic properties of LiF are taken into account. These cause a deviation from the assumed isotropic sound velocity; hence the ratio of the mean squared and cubed velocities has to be calculated. Moreover heat pulse studies⁷ have shown that, if the group velocity is not in the same direction as the wave vector, the energy flow will be enhanced, or focussed in some directions and reduced in others. McCurdy e.a.⁸ evaluated this effect for a number of cubic crystals among which LiF. For our sample, a $\langle 100 \rangle$ axis rod, with $\{100\}$ side faces⁹ the mean free path expressed in sample diameter (including the 'Casimir length' and the non isotropic velocities) is given as⁸

$$l = 1.80 d. \quad (10)$$

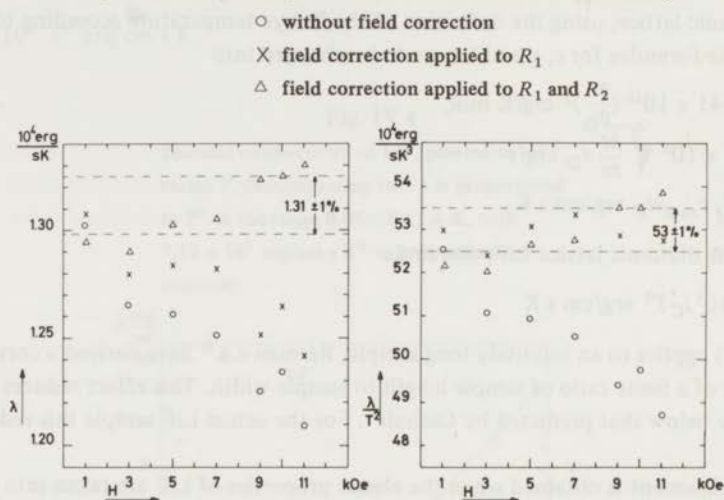
For our sample the geometric mean diameter is 0.53 cm. Combining eq. (9), (10), and the finite length correction, we find for the theoretically expected conductivity

$$\lambda = 7.14 \times 10^5 T^3 \text{ erg/cm s K},$$

which is in excellent agreement with the experimental value.

Pure LiF is diamagnetic, it is therefore a suitable substance to check the field correction on the thermometry. In fig. IV.5, the conductivity as a function of magnetic field for $T=0.5$ K is shown, it is evident that the field correction is necessary. If the measurement is performed keeping constant R_2 and applying the field correction to R_1 , then there is apparently still a field dependence in the conductivity. But this is due to measuring with constant R_2 instead of constant T_2 . If the field correction is applied to both R_1 and R_2 , the conductivity is indeed constant within the accuracy of the measurement.

Fig. IV.5
Thermal conductivity of LiF, plotted as λ and λ/T^2 versus H ,
showing the necessity of magnetic field corrections on the thermometry.



$\text{ZnSiF}_6 \cdot 6\text{H}_2\text{O}$ (sample dimensions: $3.0 \times 0.22 \times 0.25$ cm, geometry factor: 29.4 cm^{-1})

An additional calibration of the apparatus provided the measurement of a crystalline sample having a poor thermal conductivity. Comparison of the results (fig. IV.6), with those of LiF and brass (fig. IV.2, IV.4) shows that the accuracy had been improved significantly by the introduction of the automatic temperature regulation (section III.2). $\text{ZnSiF}_6 \cdot 6\text{H}_2\text{O}$ is a diamagnetic crystal of hexagonal symmetry, spacegroup $C_{3i}^2(R\bar{3})$ and, having a large number of ions in the unit cell, better comparable to the samples mentioned in section IV.3, than LiF.

The temperature dependence of λ suggests that an other scattering process than boundary scattering was important. This other process occurred down to quite low temperatures, hence it is reasonable to describe the data with boundary and dislocation scattering. If these two scattering processes occur, the conductivity may, in first approximation, be given as

$$\frac{1}{\lambda} = \frac{1}{\lambda_b} + \frac{1}{\lambda_d} \quad (11)$$

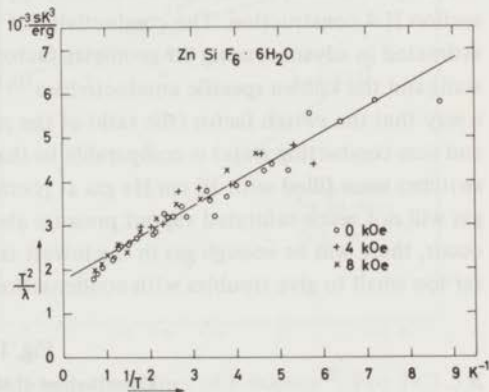
As stated in section I.1, $\lambda_b = aT^3$ and $\lambda_d = bT^2$, and consequently the conductivity will be

$$\frac{1}{\lambda} = \frac{1}{aT^3} + \frac{1}{bT^2} \quad (12)$$

In fig. IV.6, the data, fit to this relation, are shown, and eq. (12) describes the temperature dependence quite well up to about 1 K.

Fig. IV.6

Thermal conductivity of $\text{ZnSiF}_6 \cdot 6\text{H}_2\text{O}$, plotted as T^2/λ versus $1/T$, so that the value at $1/T=0$ gives the inverse of the coefficient due to dislocation scattering, and the tangent gives the inverse of the coefficient due to boundary scattering.



The experimental value of the conductivity in the boundary scattering regime

$$\lambda_b = 5.31 \times 10^4 T^3 \text{ erg/cm s K},$$

may be compared to the theory of lattice conductivity using eq. (8). For the Debye temperature we take 102 K, as found from specific heat measurements of $\text{CuSiF}_6 \cdot 6\text{H}_2\text{O}$ ¹⁰. (Since s is unknown, this θ_D has been calculated from the specific heat using the formula for a monatomic lattice.) The crystal was found to be broken parallel to its longest direction when taking it out of the sample holder, we therefore use $l=0.1$ cm instead of the sample diameter. In this case eq. (8) may be written as

$$\lambda = 2.56 \times 10^{12} \frac{1}{s} \left(\frac{\rho}{M}\right)^{2/3} \frac{1}{\theta_D^2} T^3 l \quad (13)$$

Inserting the mentioned values of λ_b , θ_D and l , $\rho=2$ g/cm³, and $M=315$ in eq. (13) yields $s=16$. This experimental value agrees rather well with $s=14$, expected on basis of the number of atoms and atomic groups in $\text{ZnSiF}_6 \cdot 6\text{H}_2\text{O}$.

In fig. IV.6, some data measured in magnetic fields of 4 kOe and 8 kOe are shown as well, and in this case, the same conclusion holds as for LiF: the field correction for the thermometry is accurate enough to show, within the accuracy of the measurement, a field independent conductivity.

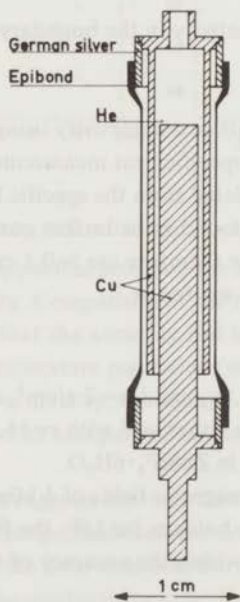
IV.2 Thermal conductivity of He gas and its use as thermal switch

Section II.4 describes the construction of a gas-switch as thermal connection between the ^3He bath and the cooling salt. As a consequence of the rather successful operation, we were interested in the actual conductivity of such a thermal switch. This section concerns the measurements on a 'mini-switch', its characteristics being comparable to the one used in section II.4.

Fig. IV.7 shows the construction of the mini-switch, in principle a copper shield and a copper pen in an epibond enclosure. The copper pen replaces the cooling salt of the section II.4 construction. The conductivity of both the epibond wall and the gas may be estimated in advance, using the geometry factors (75 for the gas and 0.04 for the epibond wall) and the known specific conductivities^{10,11}. The geometry factors were chosen in such a way that the switch factor (the ratio of the conductivities of the switch in the conducting and non conducting state) is comparable to that of a lead superconductive switch. The switches were filled with 10 cm He gas at room temperature; 10 cm because in that case the gas will not reach saturated vapour pressure above 1 K. If only few absorptions on the wall occur, there will be enough gas in the lowest temperature range, and the amount of gas is far too small to give troubles with condensation.

Fig. IV.7

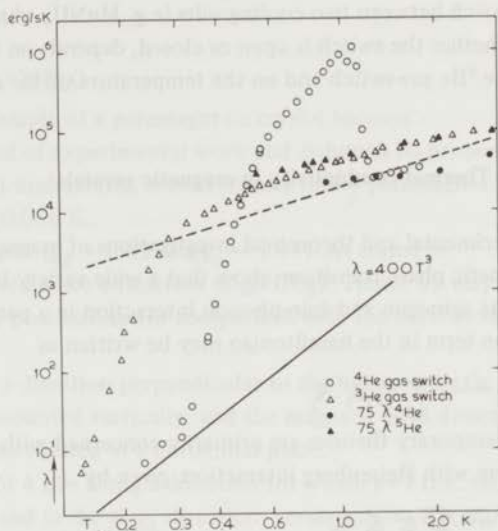
Construction of the mini-switch.



In fig. IV.8, the conductivity of the mini-switch, filled with either ^4He or ^3He , is shown.

Fig. IV.8

Thermal conductivity of the mini-switch; the values of λ for ^4He and ^3He refer to those reported by Fokkens¹⁰.



For $T > 1.3$ K the conductivity agrees quite well with the values of Fokkens¹⁰. For $T < 1.3$ K the ^3He conductivity is lower than the values reported by Fokkens¹⁰. This is probably due to the fact that both the boundary resistance and the thermal resistance of the copper pen (shield) are measured in series with the thermal resistance (i.e. the inverse conductivity) of the ^3He gas. Near 0.15 K, the lower bound, due to the conductivity along the epibond wall, is reached. The conductivity of the epibond wall was derived from the \dot{Q} versus T curve up to 0.6 K; this could be described by $\dot{Q} = aT^4$ resulting in a conductivity of $400 T^3$ erg/s K. For the ^4He filled gas-switch a remarkable rise in the conductivity occurs near 1.2 K; note that this temperature corresponds to the one where ^4He gas is expected to be at saturated vapour pressure. The rise in conductivity must be due to the onset of superfluid film flow on the epibond wall. In this case the operation of the switch is quite similar to that of a heat pipe¹². The thermal transport is a consequence of evaporation on the warm and condensation on the cold side; the superfluid film reestablishes the mass equilibrium. This process may be effective, independent of the temperature of the cold side (provided it is below a certain temperature). Hence, when measuring the \dot{Q} versus T curve in this case the temperature dependence changes near 0.35 K from T^4 to T^3 . This behaviour is probably the origin of the negative result on the ^4He gas-switch reported by Gorter¹³.

The characteristics of He filled gas-switches are summarized in the following points:

- a. The use of ^4He gas as thermal switch between a ^3He bath and a cooling salt is quite a good possibility, provided the ^3He bath is colder than 0.35 K. In the temperature range

- of interest, the switch factor can be made 100 (or more) times larger than the switch factor of lead.
- ^3He gas may be used as a thermal switch down to about 0.15 K. Hence it may serve as a switch between two cooling salts (e.g. MnNH_4 -alum and CMN).
 - Whether the switch is open or closed, depends on the temperature of the warm side for the ^4He gas-switch and on the temperature of the cold side for the ^3He gas-switch.

IV.3 Thermal conductivity in magnetic crystals

Experimental and theoretical investigations of magnetic crystals, in particular near the magnetic phase transition, show that a wide variety in behaviour may be found, depending on the spin-spin and spin-phonon interaction in a particular crystal. In general the interaction term in the hamiltonian may be written as

$$\mathcal{H}_{\text{int}} = -2 \sum_{i,j} J_{ij} \mathbf{S}_i \cdot \mathbf{S}_j$$

Contemporary theories are primarily concerned with two limiting cases, i.e. a magnetic system with Heisenberg interaction, given by

$$\mathcal{H}_H = -2J \sum_{i,j} \mathbf{S}_i \cdot \mathbf{S}_j$$

and a magnetic system with Ising interaction, given by

$$\mathcal{H}_I = -2J \sum_{i,j} S_i^z S_j^z$$

One of the important differences between the two types of interaction is that spin waves (a continuous excitation spectrum for the ordered magnetic system) may occur in crystals with the Heisenberg type interaction, but not in crystals with the Ising type interaction. The occurrence of spin waves may give rise to an alternative way for heat transport (magnon conductivity), hence a larger conductivity than that expected from lattice conductivity alone. Whether or not appreciable heat transport in the magnetic system occurs, can be investigated by thermal conductivity measurements as a function of magnetic field. In a magnetically ordered system the application of a magnetic field causes a shift, $\Delta E = g\mu H$, in the magnon energy spectrum, leading to an extra term in the Boltzmann distribution for the excitation of magnon modes. For an isotropic ferromagnet, this leads to a decrease in the number of magnons, thus a decrease in the magnon contribution to the conductivity, with increasing field; so that merely the phonon contribution survives at high magnetic field strengths.

The choice of crystals was made in a sequence of increasing complexity of the expected conductivity behaviour:

- crystals with a disordered magnetic system over the whole experimentally accessible temperature range. The band-model of section I.2 can be tested.

- b. crystals with an Ising type magnetic system, and a magnetic phase transition within the available temperature range.
- c. crystals with a Heisenberg type magnetic system, and a magnetic phase transition within the available temperature range.

Thermal conductivity of $Ce_2Mg_3(NO_3)_{12} \cdot 24H_2O$

Ce-Mg-nitrate (CMN) is chosen as an example of a paramagnetic crystal because:

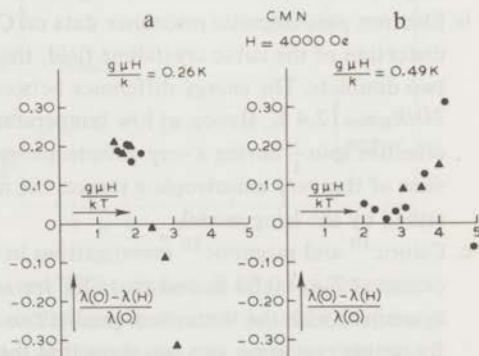
- a. CMN has been a subject of a great deal of experimental work and although its properties at ultra low temperatures are not well understood, it behaves as a spin $\frac{1}{2}$ paramagnet following Curie's law down to about 0.006 K.
- b. The g tensor in CMN is very anisotropic ($g_{\parallel} = 0.02$ and $g_{\perp} = 1.84$). As stated in section I.2, the conductivity is expected to be a function of $g\mu H/k_B T$. Hence by varying g , H , and T , one has in this case three possibilities for comparison with the band-model of section I.2.

The rod shaped samples were cut along a direction perpendicular to the hexagonal axis (=minimum g direction). The rod was mounted vertically, and the magnetic field direction (perpendicular to the heat flow) could be rotated in a horizontal plane.

In fig. IV.9, the change in λ for a field of 4 kOe along a direction for which $g=1$ (i.e. the angle between H and the c axis is 33°), and in the $g=g_{\perp}$ direction, versus $g\mu H/k_B T$ is shown. As can be seen from fig. IV.9b, merely the location of the maximum scattering, measured in the g_{\perp} direction is in moderate agreement with eq. (I.14).

Fig. IV.9

Thermal conductivity of $Ce_3Mg_2(NO_3)_{12} \cdot 24H_2O$ in a magnetic field; the direction of the field making 33° with (a) or being perpendicular to (b) the c axis.



Although many experimental runs were taken on several CMN samples, we were unable to give an adequate description of their results in terms of our simple scattering model.

Some comments on this rather disappointing conclusion can be made:

- a. The single crystals, grown from aqueous solution, are always in the form of hexagonal plates. Damage (such as cracks from cooling the sample) and crystalline defects will occur principally in planes perpendicular to the c axis. These 'defect planes' are parallel to the

heat flow, hence a favourable situation for specular reflection. This may be the origin of both the different temperature dependences (T^n with $2.5 < n < 3$) and different absolute values (differences up to a factor 10) found for different samples.

- b. Due to the small line width, the change in λ is rather small, so for a more precise analysis of the change in λ as a function of $g\mu H/k_B T$, the accuracy should be improved.
- c. All the samples, at low enough temperatures (e.g. $T < 0.2$ K) yield a conductivity in magnetic field exceeding the zero field value. This must have been due to either scattering in zero field by the magnetic system (Ce ions), which is rather unlikely; or to an additional conductivity in the magnetic system (e.g. diffusive thermal transport).

The band-model (section I.2) does not include the possibility of an increase in thermal conductivity caused by the magnetic field. For such cases, a more refined model is necessary, such as, for instance, the treatment of a paramagnetic crystal as a coupled magnetic-lattice system with magneto-elastic modes (magneto-phonons). The thermal conductivity for this model has been calculated by several authors^{14, 15, 16}. It would be interesting to repeat the measurements on CMN with an improved accuracy, to be able to make a comparison between the thermal conductivity in a (concentrated) paramagnetic crystal and the magneto-phonon theory.

Thermal conductivity of CoCs_3Cl_5 (sample dimensions: 1.5 x 0.2 x 0.35 cm)

As an example of a three dimensional (3D) Ising system we measured the thermal conductivity of CoCs_3Cl_5 (CCC). A wide variety of data are known on this substance:

- a. The crystallographic structure, spacegroup D_{4h}^{18} (I4/mcm), shows that all Co ions are magnetically equivalent, and arranged in a single Bravais lattice¹⁷.
- b. Electron paramagnetic resonance data on CCC¹⁸ show that, due to the tetragonal distortion of the cubic crystalline field, the fourfold degenerate ground state is split into two doublets. The energy difference between the two doublets amounts to $2D/k_B = -12.4$ K. Hence, at low temperatures, the Co ions may be described by an effective spin $\frac{1}{2}$ having a very anisotropic splitting factor, i.e. $g_{\parallel} = 7.20$ and $g_{\perp} = 0$. In view of this very anisotropic g tensor, the magnetic exchange interaction may be described by the Ising model.
- c. Caloric¹⁹ and magnetic²⁰ investigations in CCC show that the magnetic phase transition occurs at $T_N = 0.53$ K, and that CCC has some characteristic properties, which are in agreement with the theoretical predictions for the 3D simple cubic Ising anti-ferromagnet. By simple reasoning, one can show that the dipolar hamiltonian also simplifies to the Ising-hamiltonian in this crystal (neglecting the long range character of the dipolar interaction). Hence dipolar interaction does not affect the Ising model characteristic that spin wave excitations are absent.

Thermal conductivity was measured in a sample having its longest direction perpendicular to the c axis. During the experiment the magnetic field was along the c axis (that is the direction of the maximum $g = g_{\parallel}$ value). The direction of the c axis could be accurately

determined by means of rotating the magnetic field with respect to the crystal axis. Due to the anisotropic g value a rotation of the field caused a change of the temperature of the sample, which could be seen by the carbon thermometers. In this way it was possible to align the field along the c axis, with accuracy of 1° .

We measured the thermal conductivity as a function of temperature, in zero field as well as in 10 kOe, and further as a function of magnetic field strength at 1.703 K and 0.645 K. The results are shown in fig. IV.10, IV.11. From these data we conclude:

- There is no notable change in temperature dependence of λ near T_N . So the ordering of the magnetic system is not reflected in the thermal conductivity of this crystal.
- Within the accuracy of the measurement, the conductivity is independent of the magnetic field strength.

Fig. IV.10

Thermal conductivity of CoCs_3Cl_5
as a function of temperature.

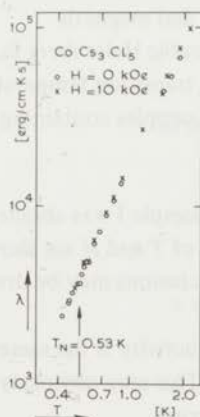
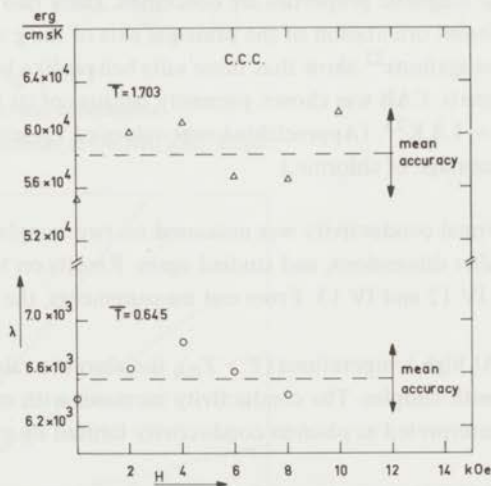


Fig. IV.11

Magnetic field dependence
of the thermal conductivity of CoCs_3Cl_5 .



Although, apparently, neither magnetic field nor the phase transition affect the thermal conductivity, the absolute value of λ is quite low. This may indicate a depression of the conductivity due to the magnetic system over the whole temperature range, in that case, both doublets need to be taken into account for an evaluation of the phonon scattering by the magnetic system. The H independence of λ may be related to the observation²⁰ that the spin-lattice relaxation is predominantly due to a Raman process, and practically independent of the magnetic field strength.

The absence of a marked variation in λ near T_N may be characteristic for the Ising model. According to Kawasaki²¹ phonon scattering by the magnetic spin system may be

proportional to the thermal conductivity of the magnetic spin system itself. As stated earlier there are no magnons in an Ising system, hence if any heat transport in the spin system occurs, this is not due to wave-like excitations but to a diffusive process. It is plausible that such a diffusive (i.e. short range) process is little dependent on T in the immediate vicinity of the phase transition temperature. Consequently, the magnetic phonon scattering is independent of T_N , and the same will be true for the thermal conductivity.

Thermal conductivity of $\text{Cu}(\text{NH}_4)_2\text{Br}_4 \cdot 2\text{H}_2\text{O}$ (sample I, dimensions: 1.95 x 0.23 x 0.23 cm; sample I abraded, dimensions: 1.95 x 0.20 x 0.20 cm; sample III, dimensions: 1.85 x 0.22 x 0.22 cm)

Copper ammonium bromide (CAB) belongs to a group of ferromagnetic salts, with the general formula $\text{CuM}_2^+(\text{Hal})_4 \cdot 2\text{H}_2\text{O}$. The crystallographic structure, spacegroup D_{4h}^{14} ($P4/mmm$), is tetragonal, and the body centered unit cell contains two Cu ions. As far as their magnetic properties are concerned, these two ions are equivalent, apart from a different orientation of the principal axis of the g tensor. Caloric and magnetic investigations²² show that these salts behave like body centered cubic Heisenberg ferromagnets. CAB was chosen primarily because of its relatively high transition temperature $T_C = 1.8 \text{ K}^{23}$. (Appreciable lower values of T_C may be found in samples containing a small percentage of chlorine.)

Thermal conductivity was measured on two samples (I and III). Sample I was abraded to smaller dimensions, and studied again. Results on λ as a function of T and H are shown in fig. IV.12 and IV.13. From our measurements, the following conclusions may be drawn.

- a. At high temperatures ($T > T_C$), the absolute value of the conductivity is the same for both samples. The conductivity increases with magnetic field. This may obviously be interpreted as phonon conductivity limited by magnetic scattering.
- b. At low temperatures ($T < 0.4 \text{ K}$), the curves are qualitatively the same. For sample III the conductivity is about 2 times lower than for sample I. Abrading sample I did not influence the conductivity, hence size dependence is not apparent in this case.
- c. For the abraded sample I, λ has been measured in 5 kOe down to 0.15 K. In the region $0.15 < T < 0.20 \text{ K}$, the data correspond to a T^3 dependence of λ , with an absolute value lower than the zero field value. Moreover, as shown in fig. IV.13, for sample III the conductivity decreases continuously with increasing magnetic field. Both field and temperature dependence suggest that magnon heat transport predominates at low temperature.

Fig. IV.12

Thermal conductivity of $\text{Cu}(\text{NH}_4)_2\text{Br}_4 \cdot 2\text{H}_2\text{O}$
as a function of temperature.

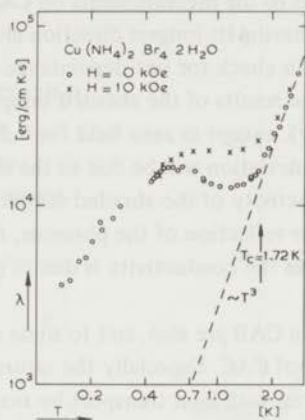
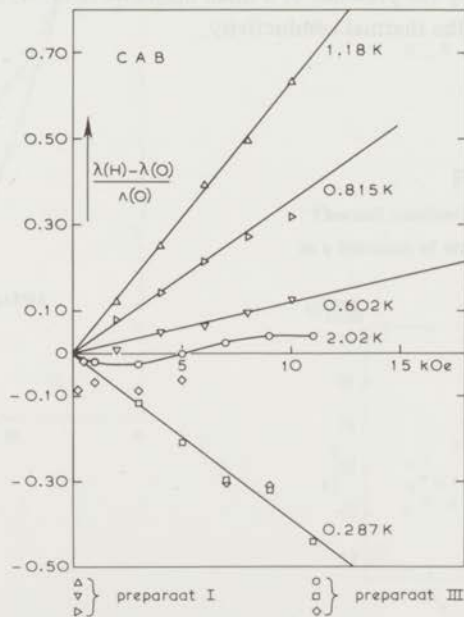


Fig. IV.13

Magnetic field dependence
of the thermal conductivity of $\text{Cu}(\text{NH}_4)_2\text{Br}_4 \cdot 2\text{H}_2\text{O}$.



Thermal conductivity of $\text{Cu}(\text{NH}_4)_2\text{Cl}_4 \cdot 2\text{H}_2\text{O}$ (sample dimensions: 1.77 x 0.23 x 0.27 cm; abraded: 1.22 x 0.14 x 0.20 cm)

Copper ammonium chloride (CAC) is another example of the '3D Heisenberg ferromagnets', having $T_C = 0.70 \text{ K}$ ²⁴. In addition to the measurements on CAB, the conductivity of CAC has been measured. The sample, having its longest direction along the *c* axis, has been measured and thereafter abraded to check for size dependence.

As can be seen from fig. IV.14, the results of the abraded sample coincide with the original curve (drawn in the figure), except in zero field for $0.3 < T < 0.6 \text{ K}$ and in 11 kOe for $T < 0.3 \text{ K}$. Especially the last deviation will be due to the size dependence of the phonon conductivity. Although the conductivity of the abraded sample is larger than the original one, which may be due to specular reflection of the phonons, this size dependence proves that, in 11 kOe at low temperatures the conductivity is due to phonons limited by boundary scattering.

The main features of the results on CAB are also, and to some extent more pronouncedly, demonstrated in the conductivity of CAC. Especially the saturation of the field effect at low temperatures, expected for a crystal with heat transport by magnons, is nicely demonstrated in the *H* dependence of the conductivity at 0.153 K and 0.177 K.

A remarkable difference in the zero field curves of CAB and CAC is the rather sharp minimum (fig. IV.16) in the conductivity of CAC at T_C . From specific heat measurements²⁴, it was found that the sharp maximum in the heat capacity, due to the phase transition, is considerably broadened by the presence of a small magnetic field. As shown in fig. IV.16, a similar effect occurs in the thermal conductivity.

Fig. IV.14
 Thermal conductivity of $\text{Cu}(\text{NH}_4)_2\text{Cl}_4 \cdot 2\text{H}_2\text{O}$
 as a function of temperature.
 The drawn line corresponds to
 the conductivity of the unabraded sample.

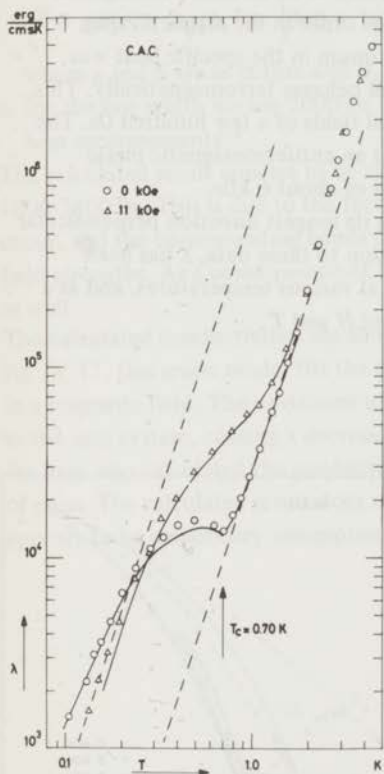


Fig. IV.15
 Magnetic field dependence
 of the thermal conductivity of $\text{Cu}(\text{NH}_4)_2\text{Cl}_4 \cdot 2\text{H}_2\text{O}$.

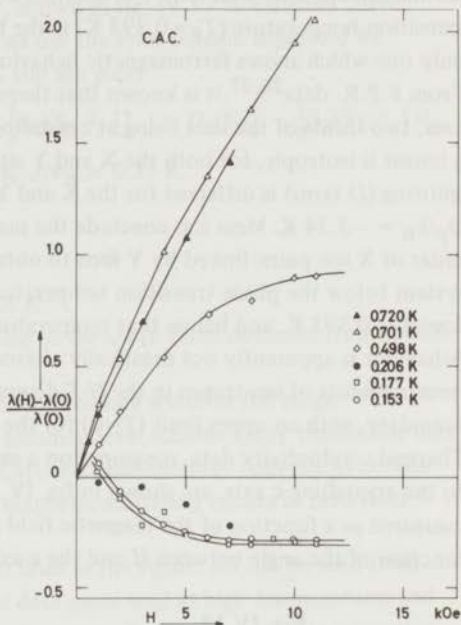
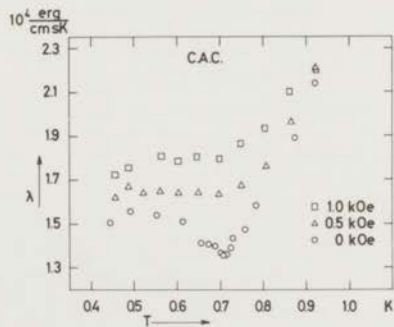


Fig. IV.16
 Thermal conductivity of $\text{Cu}(\text{NH}_4)_2\text{Cl}_4 \cdot 2\text{H}_2\text{O}$
 as a function of temperature near $T_C = 0.70 \text{ K}$.



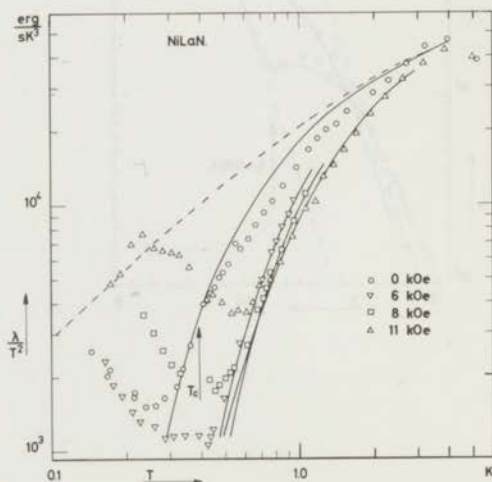
Thermal conductivity of $\text{Ni}_3\text{La}_2(\text{NO}_3)_{12}\cdot 24\text{H}_2\text{O}$ (sample dimensions: 1.6 x 0.25 x 0.26 cm)

The rare earth double nitrates have been fairly extensively investigated by various methods. Mess e.a.²⁵ investigated those double nitrates in which an iron group ion and diamagnetic lanthanum are the metal ions. For thermal conductivity, we chose NiLaN because its transition temperature ($T_C=0.393$ K) is the highest one in this group, and because it is the only one which shows ferromagnetic behaviour below its phase transition temperature. From E.P.R. data^{26,27} it is known that there are two lattice sites, X and Y, for the divalent ions, two thirds of the ions being at crystallographic X sites and one third at Y sites. The g tensor is isotropic, for both the X and Y site ions $g=2.23$. The zero field energy level splitting (D term) is different for the X and Y site ions; for NiLaN $D_x/k_B = +0.288$ K and $D_y/k_B = -3.24$ K. Mess e.a. conclude the magnetic structure to be an antiferromagnetic order of X ion pairs, linked by Y ions to obtain long range order in the magnetic spin system below the phase transition temperature. The maximum in the specific heat was found at 0.393 K, and below that temperature the crystal behaves ferromagnetically. This behaviour is apparently not drastically altered by external fields of a few hundred Oe. The measurements of isentropes in the H - T diagram²⁵ suggest an antiferromagnetic phase boundary, with an upper limit ($T=0$) for the critical field of about 6 kOe. Thermal conductivity data, measured on a sample having its longest direction perpendicular to the crystalline c axis, are shown in fig. IV.17. In addition to these data, λ has been measured as a function of the magnetic field strength H , at various temperatures, and as a function of the angle between H and the c axis at constant H and T .

Fig. IV.17

Thermal conductivity of $\text{Ni}_3\text{La}_2(\text{NO}_3)_{12}\cdot 24\text{H}_2\text{O}$.

The drawn line corresponds to the conductivities calculated with the band-model, starting from an assumed lattice conductivity (dashed curve).



From the zero field curve we note that the effect of the phase transition is a steeper T dependence of λ below T_C than above T_C . From the mentioned properties of NiLaN one may conclude that it behaves like a paramagnet for $H \geq 6$ kOe. We have calculated the conductivity on the basis of the band-model of section I.2 starting from the assumptions:

- a. an estimated 'undisturbed' lattice conductivity, shown in fig. IV.17 as a dashed curve.
- b. instead of the two-level scheme of section I.2, we use the level scheme suggested by Mess e.a.²⁵, given by the hamiltonian for the X site ion pairs:

$$\mathcal{H} = g\beta\mathbf{H}\cdot\mathbf{S}_1 + g\beta\mathbf{H}\cdot\mathbf{S}_2 - 2J\mathbf{S}_1\cdot\mathbf{S}_2 + D_x[S_{1z}^2 - \frac{1}{3}S_1(S_1 + 1)] + D_x[S_{2z}^2 - \frac{1}{3}S_2(S_2 + 1)],$$

where $S_1 = S_2 = 1$; $g = 2.23$; $D_x/k_B = 0.288$ K; $J/k_B = 0.33$ K.

And for the Y site ions

$$\mathcal{H} = g\beta\mathbf{H}\cdot\mathbf{S} + D_y[S_z^2 - \frac{1}{3}S(S + 1)]$$

where g and S are as before and $D_y/k_B = -3.24$ K²⁷.

- c. for the line width we use 2000 Oe, corresponding to the $\sqrt{b/c}$ value obtained from specific heat measurements²⁵.

The calculated result appears to be almost independent of line width in the range 1800-2400 Oe. This is due to the fact that in the assumed level scheme many transitions may occur, and the corresponding bands of strongly scattered phonons may coincide at certain field strengths. As a consequence of the D term, magnetic scattering occurs in zero field as well.

The calculated conductivities are shown as drawn lines in the figure. As can be seen from fig. IV.17, this crude model fits the experimental data quite well at high temperatures and in a magnetic field. The deviations at low temperatures may be due to magnetic saturation in the spin system, causing a decreasing line width.

We have also calculated the conductivity for the case of scattering by single X ions instead of pairs. The calculated result does not fit to the experimental data. Hence X site ion pairs appears to be a necessary assumption for interpretation of the thermal conductivity data.

References

1. W.R.G. Kemp, P.G. Klemens, R.J. Tainsh and G.K. White, *Acta Metallurgica* **6** (1957) 303.
2. C.V. Briscoe and C.F. Squire, *Phys. Rev.* **106** (1957) 1175.
3. W.W. Scales, *Phys. Rev.* **112** (1958) 49.
4. H.B.G. Casimir, *Physica* **5** (1938) 495.
5. P.H. Keesom, *Handbuch der Physik*, part 14 (1956).
6. R. Berman, F.E. Simon and J.M. Ziman, *Proc. Roy. Soc. A* **220** (1953) 171.
7. B. Taylor, H.J. Maris and C. Elbaum, *Phys. Rev. Letters* **23** (1969) 416.
8. A.K. McCurdy, H.J. Maris and C. Elbaum, *Phys. Rev. B* **2** (1970) 4077.
9. We thank Dr. B. Knook and mr. C.E. Snel for taking the röntgen diffraction pattern for us.
10. F.W. Klaaysen, private communication.
11. K. Fokkens, *Physica* **30** (1964) 2153.
12. G. Yale Eastman, *Scientific American*, May 1968, 38.
13. F.W. Gorter, Thesis Amsterdam (1969).
14. R.J. Elliot and J.B. Parkinson, *Proc. Roy. Soc. A* **92** (1967) 1024.
15. V. Roundy and D.L. Mills, *Phys. Rev. B* **1** (1970) 3703.
16. E.M. Iolin, *Soviet Phys. Solid State* **12** (1970) 905.
17. B.N. Figgis, M. Gerloch and R. Mason, *Acta Cryst.* **17** (1964) 506.
18. R.P. van Stapele, J.C.M. Henning, C.E.G. Hardeman and P.F. Bongers, *Phys. Rev.* **150** (1966) 310.
19. R.F. Wielinga, H.W.J. Blöte, J.A. Roest and W.J. Huiskamp, *Physica* **34** (1967) 223.
R.F. Wielinga, Thesis Leiden (1968).
20. K.W. Mess, E. Lagendijk, D.A. Curtiss and W.J. Huiskamp, *Physica* **34** (1967) 126.
K.W. Mess, Thesis Leiden (1969).
21. K. Kawasaki, *Pogr. Theor. Phys.* **29** (1963) 801.
22. A.R. Miedema, R.F. Wielinga and W.J. Huiskamp, *Physica* **31** (1965) 1585.
23. T.O. Klaassen, *Physica*, to be published.
24. A.R. Miedema, H. van Kempen and W.J. Huiskamp, *Physica* **29** (1963) 1266.
H. van Kempen, Thesis Leiden (1965).
25. K.W. Mess, E. Lagendijk, N.J. Zimmerman, A.J. van Duyneveldt, J.J. Giesen and W.J. Huiskamp, *Physica* **43** (1969) 165.
26. R.S. Treman, *Proc. Roy. Soc. A* **66** (1953) 118.
27. J.W. Culvahouse, *Journ. Chem. Phys.* **36** (1962) 2720.

CHAPTER V

THERMAL CONDUCTIVITY IN A 3D HEISENBERG FERROMAGNET

In the preceding chapter, thermal conductivity data were presented on a number of magnetic crystals at temperatures in the vicinity of their phase transitions. Comparison of these results show that the shapes of the conductivity versus temperature curves are quite different for the various magnetic compounds, suggesting that the actual conductivity depends on the type of magnetic interaction in a particular compound. The thermal conductivity behaviour of $\text{Cu}(\text{NH}_4)_2\text{Br}_4 \cdot 2\text{H}_2\text{O}$ and $\text{Cu}(\text{NH}_4)_2\text{Cl}_4 \cdot 2\text{H}_2\text{O}$ may therefore be representative for the conductivity of a dielectric crystal containing a 3D Heisenberg ferromagnet. This conclusion is supported by similar data on $\text{Cu}(\text{K})_2\text{Cl}_4 \cdot 2\text{H}_2\text{O}$, reported by Van Kempen¹ and Dixon e.a.². It may therefore be worthwhile to give a more detailed discussion of the thermal conductivity data on CuNH_4 chloride and -bromide. The analysis will be primarily concerned with the behaviour of the thermal conductivity at temperatures near the phase transition.

V.1 Scaling of the thermal conductivity near a magnetic phase transition

A marked difference in the zero magnetic field curves from $\text{Cu}(\text{NH}_4)_2\text{Br}_4 \cdot 2\text{H}_2\text{O}$ and $\text{Cu}(\text{NH}_4)_2\text{Cl}_4 \cdot 2\text{H}_2\text{O}$ is their behaviour near T_c : a broad minimum of λ in the bromide can be compared to a rather sharp one in the chloride.

Theoretically, the temperature dependence of the transport properties near a second order magnetic phase transition may be derived using 'dynamic scaling' arguments. We first recall the 'static scaling' concept for the thermodynamic behaviour in the critical region. Near the phase transition ($T \rightarrow T_c$), several properties of the magnetic system diverge (e.g. specific heat, susceptibility). The character of the divergence may be expressed by a function of the variable $\epsilon = |T - T_c|/T_c$, so that a divergent observable f may be characterized by the 'critical exponent' p of the leading term in the singularity for $\epsilon \rightarrow 0$, hence

$$f(\epsilon) \sim \epsilon^{-p}. \quad (1)$$

A number of critical exponents have been defined in order to characterize equilibrium (static) properties (see e.g. ^{3,4}). These exponents are of interest because of the similarity of physical systems near the critical point.

A key to the present understanding of equilibrium behaviour near T_c is the realization, that the thermodynamic derivatives, expressed as correlation functions, are related to the fluctuations in the system. The number of particles (e.g. magnetic spins) involved in a fluctuation, diverges as T approaches T_c . The fluctuations may be characterized by a correlation length ξ , which in turn diverges and is given by

$$\xi = r_0 \epsilon^{-\nu} \quad (2)$$

where r_0 is some characteristic length, e.g. the lattice parameter in a magnetic spin system and ν is the ξ characterizing exponent.

The crucial assumption in 'static scaling' is that, in spite of the complexity of the phase transition, the thermodynamic derivatives may be characterized by the single parameter ξ . Put in another way, the correlation function expression for a particular thermodynamic quantity, which is in general a function of the distance r or the wavenumber k , is assumed to be a homogeneous function in r/ξ or $k\xi$. In order to describe transport properties, the static scaling assumption is extended to the frequency domain (see e.g.^{3,5,6}). A transport coefficient is proportional to a time dependent correlation function, which may be characterized by a frequency as well as a length. That frequency is expected to diverge ('slowing down') near T_c , and in 'dynamic scaling', it is assumed to be a homogeneous function of $k\xi$ as well.

To calculate the temperature dependence of transport properties, one proceeds as follows. The macroscopic laws of motion (hydrodynamic-equations) are valid in the region $k\xi \ll 1$; since ξ depends on T through ϵ , $k\xi \ll 1$ implies two regions: the ordered, $T < T_c$, and the disordered, $T > T_c$, region. On the other hand, in the region $k\xi \gg 1$, the macroscopic laws break down, i.e. the transport coefficients, entering the macroscopic laws, become wave vector and/or frequency dependent. The 'dynamic scaling' assumption serves as a matching condition in the k - ξ plane at $k\xi = 1$. Therefore, when measuring a transport property near the phase transition, it is important to know the value of $k\xi$.

We now turn our attention to the specific case of thermal conductivity in a magnetic crystal near the phase transition. It should be realized that the phase transition is studied by the scattering of phonons, and in particular those phonons which are dominant in the thermal transport process. In the case of thermal conductivity in dielectric crystals, the dominant phonons therefore determine the relevant k value. If we assume that $T_c = 1$ K, that the conductivity is measured near T_c , and that the velocity of sound is 2×10^5 cm/sec, then the dominant phonon argument leads to a wavelength of about 30 lattice spacings. We are interested in the boundary between the hydrodynamic and the critical region $k\xi = 1$, this condition leads to $\xi = 30 r_0$. Using eq. (2), with $\nu = \frac{2}{3}$, we find the boundary to be given by $\epsilon \approx 10^{-2}$. For $T_c > 1$ K the value of k , and consequently ϵ , will be larger; thus the critical region may become manifest as a contribution to the phonon scattering which is not a function of ϵ . If, on the other hand, $T_c < 1$ K, ϵ will be smaller and, as far as thermal conductivity measurements with the mentioned temperature resolution are concerned, the

behaviour of λ can be interpreted on basis of the hydrodynamic equations up to $T = T_c$, i.e. the phonon scattering is a function of ϵ up to $T = T_c$.

Whether or not the preceding argument is the correct explanation of the difference in behaviour of λ in $\text{Cu}(\text{NH}_4)_2\text{Cl}_4 \cdot 2\text{H}_2\text{O}$ and $\text{Cu}(\text{NH}_4)_2\text{Br}_4 \cdot 2\text{H}_2\text{O}$, a possible divergence in λ near T_c is more likely to be seen in the thermal conductivity of the chloride than in that of the bromide. The following discussion pertains therefore in particular to the data of $\text{Cu}(\text{NH}_4)_2\text{Cl}_4 \cdot 2\text{H}_2\text{O}$.

Since thermal conductivity data near T_c are rather scarce, it is uncertain from an experimental point of view, whether or not a power law analysis is valid (recently Senger e.a.⁷ reported a successful analysis in terms of a power law for λ in CO_2). On the other hand, quite accurate data have been reported on ultrasonic attenuation near a magnetic phase transition⁸; and as far as the longitudinal modes are concerned the attenuation (a_k) was found to be described by

$$a_k \sim \omega^2 \epsilon^{-p}. \quad (3)$$

For transverse modes the divergence in the attenuation, if any, was found to be weaker, and less pronounced than for the longitudinal modes. Theoretical p values, depending on the particular magnetic ordering, anisotropy, and coupling of the sound waves to the magnetic spin system^{6,8}, range between 0 and 5/3. In a review article, Lüthi e.a.⁸ show that the critical longitudinal sound attenuation in rare earth metals can be nicely accounted for by the present theories, however in the case of magnetic insulators, the situation is less satisfactory. In fact the experimental results on ultrasonic attenuation in magnetic insulators yield p values which are considerably lower than 1.

In thermal conductivity experiments, the phonon frequencies are $10^2 - 10^4$ times larger than in the usual ultrasonic experiments. Moreover, heat transport in solids may be mainly determined by the transverse modes. Disregarding these differences between ultrasonic attenuation and thermal conductivity, i.e. assuming the ω^2 dependence to be valid, together with a strong intra-phonon coupling to restore the thermal equilibrium between the transverse and longitudinal modes, eq. (3) may be used in an analysis of λ .

The relaxation time τ_k for phonon scattering by the magnetic system is related to the ultrasonic attenuation by

$$\tau_k = v_k a_k. \quad (4)$$

If boundary and magnetic scattering are present, λ may be expressed by (Debye model, see section I.

$$\lambda = AT^3 \int_0^\infty \frac{x^4 e^x}{(e^x - 1)^2} \frac{dx}{1 + Bx^2 T^2 (\epsilon^p + C)^{-1}}. \quad (5)$$

The constant C accounts for the fact that the actual conductivity is non zero at $T = T_c$. A comparison of the undisturbed lattice conductivity of $\text{Cu}(\text{NH}_4)_2\text{Cl}_4 \cdot 2\text{H}_2\text{O}$, i.e. the extra-

polated T^3 dependence of λ ($H=11$), with the actual conductivity near T_c shows that the magnetic scattering reduces the conductivity by about a factor 15. Hence, for the purpose of discussion, we may neglect the boundary scattering, and eq. (5) simplifies to

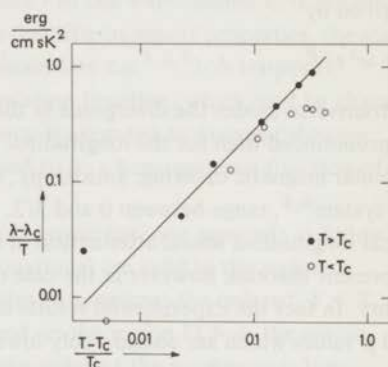
$$\lambda \sim T(\epsilon^p + C). \quad (6)$$

C may be found from the value λ_c of λ at $T = T_c$, and consequently

$$\frac{\lambda - \lambda_c}{T} \sim \epsilon^p. \quad (7)$$

As can be seen in fig. V.1, this relation fits the data (those of section IV, fig. IV.15) fairly well. It is evident that more data for $\epsilon < 0.1$ are necessary to give a reliable estimate of p ; the drawn line corresponds to $p = 1$.

Fig. V.1
Thermal conductivity of $\text{Cu}(\text{NH}_4)_2\text{Cl}_4 \cdot 2\text{H}_2\text{O}$ near T_c
plotted as $\lambda - \lambda_c/T$ versus $T - T_c/T_c$.



In the preceding analysis of λ , the variation of ϵ , i.e. T , corresponds to a variation of the phonon spectrum; it is uncertain whether this affects the resultant p value. The 'scaling law' predictions have usually been restricted to the situation of zero magnetic field and then the variable ϵ serves as a measure of the deviation from the transition point. However, at $T=T_c$, in the presence of a field H , $H - H_c$ (where for a ferromagnet $H_c=0$), is a measure of the deviation from the transition point as well. Hence measuring at constant temperature (i.e. constant phonon spectrum), and using H as a variable, a more reliable test of 'scaling law' predictions can be made. (Compare with ⁷, where a scaling law analysis of λ of CO_2 is reported as a function of T and ρ .) As can be seen from fig. IV.13 and IV.16, in low magnetic fields and far from T_c , the field dependence of the conductivity is linear in H . On the other hand, near T_c the resultant curve (fig. IV.16) is definitely convex. Hence a power law analysis, similar to the one given by Sengers e.a.⁷ for λ in CO_2 , may be made by subtracting the 'back ground H dependence' from the total H dependence at $T=T_c$. It is evident that more measurements are necessary to realize such an analysis.

V.2 Thermal conductivity near a magnetic phase transition, comparison with a microscopic model

The analysis in the preceding section is mainly phenomenological. A quite different approach would be a comparison between the experimental data, and a theoretical calculation of the conductivity, starting from a certain spin-phonon interaction. Kawasaki⁹ and Stern¹⁰ derived formulae for the thermal conductivity in a magnetic crystal, where the magnetic spin system is described by a nearest neighbour Heisenberg exchange interaction, and where the phonons couple to the spin energy density. In such a magnetic crystal, the thermal expansion coefficient is proportional to the specific heat. This has actually been found for $\text{CuK}_2\text{Cl}_4 \cdot 2\text{H}_2\text{O}$ ¹¹. Hence one may expect that also Cu-NH_4 -chloride and -bromide (isomorphous with the K-salt) represent the same model.

Both, the derivation of Kawasaki and the refined one of Stern, lead to the same conclusion: in first order, the phonon-spin energy density coupling gives rise to an inverse phonon relaxation time proportional to the thermal conductivity λ_s of the spin system, or to the specific heat c_s of the spin system, when second order effects of the phonon-spin energy density coupling are taken into account. Hence, two scattering processes are considered: first, the absorption and emission of phonons by the spin system ('direct process'), and second, the scattering of phonons by critical fluctuations in the energy density. Kawasaki's formulae, evaluated for $\text{Cu}(\text{NH}_4)_2\text{Cl}_4 \cdot 2\text{H}_2\text{O}$, lead to the mean free path expressions

$$l_1 = 2.3 \times 10^5 / a^2 T^3 \lambda_s \text{ cm}, \quad (8)$$

and

$$l_2 = 3.3 \times 10^{16} / a^4 T^6 c_s \text{ cm}, \quad (9)$$

where a is a measure of the spin-phonon interaction strength, being defined as the logarithmic derivative of the exchange energy J with respect to the interionic distance r :

$$a = \partial \ln J / \partial \ln r. \quad (10)$$

As stated in the previous section for the purpose of discussion, merely the magnetic part of the phonon scattering needs to be taken into account. Hence, with the use of

$$\lambda = AT^3 l, \quad (11)$$

a comparison between the mentioned mean free path estimates and the observed conductivity may be made.

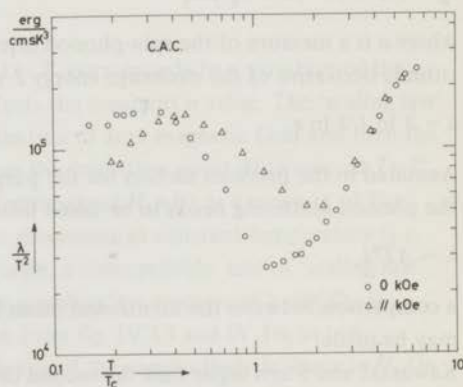
Kawasaki and Stern argue that the second order process is responsible for the behaviour of λ near T_c such as found for CoF_2 ; we therefore start with a discussion of l_2 . The specific heat of $\text{Cu}(\text{NH}_4)_2\text{Cl}_4 \cdot 2\text{H}_2\text{O}$ has been experimentally determined by Van Kempen¹, showing the specific heat to be proportional to T^{-2} above $1.3 T_c$. Hence, using eq. (9) and eq. (11), λ is expected to be proportional to T^{-1} above $1.3 T_c$. Since this is evidently not corroborated

by our experimental results (see fig. V.2 and fig. IV.14), the conductivity is not limited by the l_2 -determining scattering mechanism. We therefore turn our attention to eq. (8), and remark that the influence of the first order process depends on the behaviour of the thermal conductivity λ_s in the spin system. When the thermal transport in the spin system is regarded as a diffusive process, hence depending on short range correlations, λ_s is expected to show a mild temperature dependence in the vicinity of T_c . Under this assumption, Kawasaki evaluated λ_s , and inserting the parameters pertaining to $\text{Cu}(\text{NH}_4)_2\text{Cl}_4 \cdot 2\text{H}_2\text{O}$ we obtain

$$\lambda_s = 23 T^{-2} \text{ erg/cm s K.} \quad (12)$$

As stated in section IV.3, heat transport in the spin system is evident below 0.4 K, and it is therefore quite reasonable to assume λ_s to be non-negligible even in the vicinity of T_c . Substitution of eq. (12) and (8) into eq. (11) predicts a thermal conductivity proportional to T^2 . The experimental conductivity tends towards a T^2 -proportionality above T_c (see fig. V.2). Using the extrapolated value of λ/T^2 for $T \downarrow T_c$ we find $l = 0.011 T^{-1} \text{ cm}$. Equating this experimental mean free path to l_1 , it follows that $|a| = 950$ (due to a somewhat different analysis of the data, this a value is slightly different from that reported in ¹²). Inserting this value of a , and the 'high temperature' c_s^{-1} we find $l_2 = 0.6 T^4 \text{ cm}$. This is in agreement with the previous discussion where l_2 was rejected on basis of the temperature dependence of the conductivity. On the other hand, for $T=T_c$ we find $l_1 = 0.016 \text{ cm}$ and $l_2 = 0.24 \text{ cm}$, thus near T_c the 'critical scattering' presumably gives rise to an additional scattering of about 7%, which roughly corresponds to $\lambda(H=0.5) - \lambda(H=0)$. See fig. IV.16.

Fig. V.2
Thermal conductivity of $\text{Cu}(\text{NH}_4)_2\text{Cl}_4 \cdot 2\text{H}_2\text{O}$
plotted as λ/T^2 versus T/T_c .



Kawasaki derived $|a| = 30$ for CoF_2 and $a = -3.6$ for MnF_2 , hence our value of $|a|$ may be surprisingly large. Equation (10) defining a , may be written as

$$a = (\partial \ln J / \partial T) (\partial \ln r / \partial T)^{-1} \quad (13)$$

Recently both the temperature dependence of J^{13} and the linear thermal expansion along the a axis¹¹ have been reported for $\text{CuK}_2\text{Cl}_4 \cdot 2\text{H}_2\text{O}$. Inserting the reported values, we find for Cu-K-chloride $|a| \approx 300$ at $T=T_c$ and $|a| \approx 10^3 T^2$ for $T > T_c$, and these values are, at least in order of magnitude, in agreement with our value.

In conclusion we may say that above T_c , Kawasaki's theory describes our data quite well. A numerical calculation, based on a formula similar to eq. (5), showed this conclusion to be correct in the region close to T_c only. Actually, for T considerably above T_c , a calculation of λ under the influence of a paramagnetic system would be more appropriate. For the case of strong spin-phonon coupling, calculations have been made for the thermal conductivity of the coupled excitations (magneto-phonons), the coupling mechanism being similar to that used by Kawasaki. In the calculation by Roundy *et al.*¹⁴, pertaining to a two level spin system e.g. $S = \frac{1}{2}$ (like Cu^{2+}) in a magnetic field, it is shown that, if the dominant scattering is due to fluctuations in the spin density, λ will be proportional to T^3 , with a proportionality constant less than the one appropriate to boundary scattering alone. As can be seen in fig. IV.12 and IV.14, the thermal conductivity of $\text{Cu}(\text{NH}_4)_2\text{Br}_4 \cdot 2\text{H}_2\text{O}$ and $\text{Cu}(\text{NH}_4)_2\text{Cl}_4 \cdot 2\text{H}_2\text{O}$ in the presence of a magnetic field tends to a T^3 dependence at the high temperature side of the curve. Although it is not certain whether Roundy's calculation is valid in the zero field limit, the zero field conductivities of the two copper salts are also proportional to T^3 in the region $1.6 T_c$ to $2.5 T_c$. It is evident that at this stage, a detailed numerical calculation is necessary to conclude whether this theoretical model gives a satisfactory description of the data above T_c .

For $T < T_c$, Kawasaki's theory does not account for the data; one may speculate, this to be due to the assumption that λ_s is a smooth function of T around T_c . Since the lattice conductivity is derived to be inversely proportional to λ_s , the experimental data suggest a sudden change in λ_s at T_c . As stated before, below 0.4 K, λ_s accounts at least for an appreciable part of the total thermal transport: it is therefore unlikely that λ_s decreases below T_c . Hence our conclusion of a sudden increase of λ_s below T_c . According to eq. (8), an increase in λ_s corresponds to a decrease in the lattice conductivity. (This may be the explanation of the behaviour of $\lambda(H=0)$ in NiLa-nitrate in the vicinity of T_c , see section IV.3.) Actually, the experimental data show an increase of the total conductivity below T_c . We therefore suggest that the thermal transport below T_c is entirely due to transport in the magnetic spin system.

For thermal transport in an ordered magnetic system, using spin wave theory, the calculation of magnon conductivity may be made according to a derivation quite similar to the one for phonon conductivity. In the low temperature region, where the magnetic specific heat is proportional to $T^{3/2}$, the thermal conductivity may be expressed by¹⁵

$$\lambda_s = 0.765 \frac{k_B l}{h 2 J S r_0^2} T^2, \quad (14)$$

where l is the magnon mean free path, leading in the case of $\text{Cu}(\text{NH}_4)_2\text{Cl}_4 \cdot 2\text{H}_2\text{O}$ to

$$\lambda_s = 7.5 \times 10^8 l T^2 \text{ erg/cm s K.} \quad (15)$$

Referring to fig. V.2, λ_s is proportional to T^2 below $0.35 T_c$, and the absolute value substituted in eq. (15) yields $l = 2.0 \times 10^{-4}$ cm.

Some remarks on this result may be made.

- a. The specific heat of the spin system should be proportional to $T^{3/2}$ in order to yield a $\lambda_s \sim T^2$ relation. Heat capacity measurements below $0.2 T$ were found to give $c_s \sim T^{3/2}$ indeed. λ_s being proportional to T^2 between $0.2 T_c$ and $0.35 T_c$ may have no special significance.
- b. Since $\lambda_s \sim T^2$ corresponds to magnon boundary scattering, the resulting mean free path (2×10^{-4} cm) is probably the one for phonons as well. In that case, the lattice conductivity, about $500 T^3$, is negligible indeed, compared to the total (experimental) conductivity of $1.5 \times 10^5 T^2$.
- c. The resulting mean free path cannot be due to scattering at the sample boundaries (size effect). We suggest the scattering to be due to the ferromagnetic domains, present in the crystal. This explanation is supported by the low field behaviour of the conductivity. As can be seen from fig. IV.17, small fields ($H < 300$ Oe) cause an increase in the conductivity. This behaviour may be expected for scattering at domain boundaries, since, in weak applied fields, the volume of the domains increases with increasing magnetic field, up to a single domain as large as the sample itself.

In the preceding section an analysis has been made of the thermal conductivity data of one of our samples (i.e. CuNH_4 -chloride), from the point of view of a rather transparent theoretical model. Although far more sophisticated theories could have been used for comparison with the experimental data, it does not make sense to give a detailed analysis before knowing the qualitative behaviour of the thermal conductivity near a phase transition. We therefore confined ourselves to a qualitative analysis of the data. However, one may hope that some features are characteristic for the thermal conductivity in a 3D Heisenberg ferromagnet.

References

1. H. van Kempen, Thesis Leiden (1965).
2. G.S. Dixon and D. Walton, Phys. Rev. **185** (1969) 735.
3. P.P. Craig and W.I. Goldberg, Journ. Appl. Phys. **40** (1969) 964.
4. M.E. Fisher, Rep. Progr. Phys. **30** (1967) 615.
5. B.I. Halperin and P.C. Hohenberg, Phys. Rev. **177** (1969) 952.
6. K. Kawasaki, Journ. Appl. Phys. **41** (1970) 1311.
7. J.V. Sengers and P.H. Keyes, Phys. Rev. Letters **26** (1971) 70.
8. B. Lüthi, T.J. Moran and R.J. Pollina, J. Phys. Chem. Solids **31** (1970) 1741.
9. K. Kawasaki, Progr. Theor. Phys. **29** (1963) 801.
10. H. Stern, J. Phys. Chem. Solids **26** (1965) 153.
11. J.W. Philp and E.D. Adams, Journ. Low. Temp. Phys. **2** (1970) 309.
12. J.N. Haasbroek and W.J. Huiskamp, Phys. Lett. **33A** (1970) 173.
13. T. Okuda and M. Date, Journ. Phys. Soc. Japan **28** (1970) 308.
14. V. Roundy and D.L. Mills, Phys. Rev. **B1** (1970) 3703.
15. D. Douthett and S.A. Friedberg, Phys. Rev. **121** (1961) 1662.

CONCLUDING REMARKS

We have demonstrated in this thesis the use of thermal conductivity measurements for the study of excitations in a magnetic spin system. It is evident that analysis would be facilitated if more transport properties (e.g. ultrasonic attenuation, spin diffusion coefficient) of the crystals were known. Nevertheless, it is perhaps worthwhile mentioning several conclusions which may be drawn from our measurements, in particular those with implications for further research.

1. The thermal conductivity is shown to be influenced by magnetic excitations and, near the phase transition, it is sensitive to the type of interaction in the magnetic spin system.
2. The thermal conductivity of $\text{Cu}(\text{NH}_4)_2\text{Cl}_4 \cdot 2\text{H}_2\text{O}$ and $\text{Cu}(\text{NH}_4)_2\text{Br}_4 \cdot 2\text{H}_2\text{O}$ (representing the 3D Heisenberg ferromagnet) near the phase transition may be described by scaling law relations. The critical region is probably reflected in the conductivity of the bromide. Further experiments are necessary to support this conclusion. It is desirable to involve the magnetic field dependence of the conductivity at T_c in both the experiments and the theoretical treatment on this problem.
3. In view of the results with the copper salts, it would be quite interesting to investigate the conductivity of 3D Heisenberg antiferromagnets such as for instance $\text{Rb}_2\text{MnCl}_4 \cdot 2\text{H}_2\text{O}$ and $\text{Cs}_2\text{MnCl}_4 \cdot 2\text{H}_2\text{O}$. The points of view presented in V.1,2 should be valid in these salts as well.
4. We found the thermal conductivity to be independent of the phase-transition in an Ising antiferromagnet (CoCs_3Cl_5). This has to be confirmed with thermal conductivity measurements on other salts representing the Ising model such as for instance CoCs_3Br_5 and DyPO_4 .
5. The thermal conductivity of $\text{Ni}_3\text{La}_2(\text{NO}_3)_{12} \cdot 24\text{H}_2\text{O}$ in large magnetic fields can be described assuming Ni ion pairs. It is worth investigating the thermal conductivity of $\text{Cu}(\text{NO}_3)_2 \cdot 3\text{H}_2\text{O}$, since the existence of Cu ion pairs should be reflected in the thermal conductivity of this salt as well.
6. The thermal conductivity of $\text{Ce}_2\text{Mg}_3(\text{NO}_3)_{12} \cdot 24\text{H}_2\text{O}$ in magnetic fields is still a problem to be solved.
7. We have shown the thermal conductivity of $\text{Cu}(\text{NH}_4)_2\text{Cl}_4 \cdot 2\text{H}_2\text{O}$ and $\text{Cu}(\text{NH}_4)_2\text{Br}_4 \cdot 2\text{H}_2\text{O}$ at low temperatures to be largely determined by magnons. It would be worthwhile to investigate magnon scattering processes in these salts.

In this thesis we have attempted to summarize, from an experimental point of view, our present understanding of the influence of a magnetic spin system on the thermal conductivity. Many questions are still unanswered, but we are convinced that the solution of these problems would greatly benefit from further measurements of thermal conductivity at very low temperatures.

CONCLUDING REMARKS

We have demonstrated in this study the use of thermal conductivity measurements for the study of reactions in a magnetic spin system. It is evident that further work is indicated in some important properties for a systematic treatment. This includes the study of the system with a variety of different spin systems. It is further suggested that the present study be extended to include the study of the system with other than our measurements. In particular, there will be indicated for further work.

1. The thermal conductivity is shown to be affected by magnetic excitations and, since the spin system is a function of the type of reaction in the magnetic spin system.

2. The thermal conductivity of $\text{CaMg}_2\text{Si}_2\text{O}_8$, $\text{CaMg}_2\text{Si}_2\text{O}_8$ and $\text{CaMg}_2\text{Si}_2\text{O}_8$ is shown to be affected by the spin system and the phase transition may be identified by using the spin system. The critical region is probably related to the conductivity of the spin system. Further experiments are necessary to support the conclusion. It is desirable to study the magnetic spin system of the conductivity at T_c to both the experiment and the theoretical treatment of the spin system.

3. In view of the results with the spin system, it would be quite interesting to investigate the conductivity of $\text{CaMg}_2\text{Si}_2\text{O}_8$ in various configurations such as for instance $\text{CaMg}_2\text{Si}_2\text{O}_8$ and $\text{CaMg}_2\text{Si}_2\text{O}_8$. The points of view presented in V. 1.3 should be taken in these cases as well.

4. We have shown the thermal conductivity to be dependent of the phase transition in an important manner. The data to be compared with the thermal conductivity measurements are given in this paper. The data to be compared with the thermal conductivity measurements are given in this paper. The data to be compared with the thermal conductivity measurements are given in this paper.

5. The thermal conductivity of $\text{CaMg}_2\text{Si}_2\text{O}_8$ is shown to be dependent of the spin system. It is shown that the thermal conductivity of $\text{CaMg}_2\text{Si}_2\text{O}_8$ is dependent of the spin system. It is shown that the thermal conductivity of $\text{CaMg}_2\text{Si}_2\text{O}_8$ is dependent of the spin system. It is shown that the thermal conductivity of $\text{CaMg}_2\text{Si}_2\text{O}_8$ is dependent of the spin system.

6. The thermal conductivity of $\text{CaMg}_2\text{Si}_2\text{O}_8$ is shown to be dependent of the spin system. It is shown that the thermal conductivity of $\text{CaMg}_2\text{Si}_2\text{O}_8$ is dependent of the spin system. It is shown that the thermal conductivity of $\text{CaMg}_2\text{Si}_2\text{O}_8$ is dependent of the spin system. It is shown that the thermal conductivity of $\text{CaMg}_2\text{Si}_2\text{O}_8$ is dependent of the spin system.

7. We have shown the thermal conductivity of $\text{CaMg}_2\text{Si}_2\text{O}_8$, $\text{CaMg}_2\text{Si}_2\text{O}_8$ and $\text{CaMg}_2\text{Si}_2\text{O}_8$ to be dependent of the spin system. It is shown that the thermal conductivity of $\text{CaMg}_2\text{Si}_2\text{O}_8$ is dependent of the spin system. It is shown that the thermal conductivity of $\text{CaMg}_2\text{Si}_2\text{O}_8$ is dependent of the spin system. It is shown that the thermal conductivity of $\text{CaMg}_2\text{Si}_2\text{O}_8$ is dependent of the spin system.

In this study we have attempted to demonstrate that an experimental study of spin system is indicated. It is shown that the thermal conductivity of $\text{CaMg}_2\text{Si}_2\text{O}_8$ is dependent of the spin system. It is shown that the thermal conductivity of $\text{CaMg}_2\text{Si}_2\text{O}_8$ is dependent of the spin system. It is shown that the thermal conductivity of $\text{CaMg}_2\text{Si}_2\text{O}_8$ is dependent of the spin system. It is shown that the thermal conductivity of $\text{CaMg}_2\text{Si}_2\text{O}_8$ is dependent of the spin system.

